A STUDY OF THE VORTEX FLOW PHENOMENON

AS APPLIED TO CORNER-FIRED FURNACE

by

Gérard P. Desbois

A RESEARCH THESIS

IN THE

FACULTY OF ENGINEERING

Presented in partial fulfilment of the requirements for the

Degree of MASTER OF ENGINEERING

at

Sir George Williams University

Montreal, Canada

14th August, 1970

ACKNOWLEDGEMENTS

ABSTRACT

A mathematical model describing the flow pattern in systems similar to corner-fired furnace, with fluid having constant physical properties, is proposed.

The system is divided into three zones: the plane-free jet zone, the vortex zone and the decaying-swirl zone. For each zone the appropriate existing theory describing the flow pattern is selected and the output variables of one zone are used as input variables in the following zone.

Starting with the plane-free jet zone it is shown that the flow does not become fully developed before reaching the vortex zone and consequently an equivalent velocity is derived using the principle of momentum flux conservation. In the vortex zone the work of Kwok is used in conjunction with Burger's one-cell solution, and closed form solutions are obtained for the velocity components profiles. In the decaying-swirl zone the analytical investigation of incompressible turbulent swirling flow by Rochino and Lavan is followed and the numerical solution of the swirl equation presented.

Numerical results from the mathematical model have been computed and expressed in graphical form showing the effect of the independent parameters: fluid mass flow, inlet nozzles width and height, size of chamber and nozzle orientation, on the flow pattern of the system.

TABLE OF CONTENTS

Page

LIST OF SYMBOLS

Symbol	Definition
A_n $(n = 1,2,...)$	Constant of integration
b	Nozzle width, ft.
C	Constant of proportionality in equation (35)
d	Length of free-jet motion, ft.
E	Dimensionless eddy viscosity, $= \dfrac{e_{m(\phi)}}{\gamma}$
$e_{m(r)}, e_{m(\phi)}, e_{m(z)}$	Kinematic eddy viscosity in the radial, tangential and axial direction, ft²/sec.
H	Defined after equation (53)
h	Inlet nozzle height, ft.
K	Constant of proportionality in equation (64)
k	Constant of proportionality in equation (37)
L	Length scale in the turbulent flow field, ft.
l	Mixing length
$\dot{M}$	Momentum flux per unit length of nozzle height, slug/sec²
N	Number of inlet nozzles
P	Dimensionless pressure, $= \dfrac{\bar{P}}{\rho V^2}$
$\bar{P}$	Time-mean pressure, psf
Q	Fluid flow rate, ft3/sec
R	Half-furnace side, ft
Re	Apparent Reynold's number, $= \dfrac{VR}{\gamma_a}$
$(Re)_z$	Axial Reynold's number, $= \dfrac{\bar{V}_a R}{\gamma}$
r, ϕ, z	Cylindrical coordinates

LIST OF SYMBOLS (cont'd)

Symbol	Definition

$\bar{U}_x$, d — An average jet velocity, $= \sqrt{\int_{-\infty}^{\infty} \bar{u}\, dy}$, ft/sec.

$\bar{u}, \bar{v}, \bar{w}$ — Time-mean component of velocity in cartesian coordinates, ft/sec

u', v', w' — Fluctuating components of velocity in cartesian coordinates, ft/sec

$\bar{u}$ — Time-mean velocity component parallel to axis of jet, ft/sec.

u_m — Time-mean velocity component on the jet axis, ft/sec.

V — Tangential velocity component at inlet of vortex zone, ft/sec

$\bar{V}a$ — Average axial velocity in the decaying swirl zone, $= \dfrac{Q}{\pi R^2}$, ft/sec

Vj — Average velocity at nozzle outlet, ft/sec

Vr, V_ϕ, Vz — Dimensionless velocity in the radial, tangential and axial directions

$\bar{V}r, \bar{V}_\phi, \bar{V}z$ — Time-mean velocity components in cylindrical coordinates, ft/sec

v_r', v_ϕ', v_z' — Fluctuating components of velocity in cylindrical coordinates, ft/sec

$\underline{v}'$ — Fluctuating velocity vector

W — Effective width of jet at periphery of vortex zone, ft.

X — Dimensionless radial coordinate, $= \dfrac{r}{R}$

x, y, z — Cartesian coordinates

Z — Dimensionless axial coordinate, $= z/R$

α — Dimensionless parameter, $= \dfrac{Q}{2\pi r_a h}$

List of Symbols (Cont'd)

Symbol	Definition
β	Dimensionless parameter, $= -\dfrac{N\,(bW)^{1/2}}{2\sqrt{2}\,\eta\,R\,\sin\gamma}$
γ	Angle between nozzle axis and furnace diagonal, radian
δ	Angle subtended at furnace center by a perpendicular to furnace diagonal and originating at the intersecting point of nozzle axis and furnace inscribed circle, radian
ϵ	Eddy viscosity, lb.sec/ft^2
θ	Jet half-angle, radian
λ	Angle between jet axis and vortex diameter, radian
μ	Molecular viscosity, lb.sec/ft^2
ν	Kinematic viscosity, ft^2/sec.
ν_a	Apparent Kinematic viscosity, ft^2/sec.
ρ	Mass density, slug/ft^3
$\sigma_{x,y,z}$	Normal stress, psf
τ	A function of X = X^2 for $0 \leqslant x \leqslant 0.9$ $= (1-X)^2$ for $0.9 < x \leqslant 1.0$
τ_{s,x_1,x_3,y_3}	Turbulent shear stress, psf.
Γ	Dimensionless angular momentum, $= X V_\phi$

Subscript

i	Grid point number in the radial direction
r, ϕ, z	Indicates radial, tangential and axial direction
x, y, z	Indicates cartesian coordinate direction

LIST OF SYMBOLS (cont'd)

Superscript

j   Grid point number in the axial direction

'   FLuctuating flow variables

A STUDY OF THE VORTEX FLOW PHENOMENON

AS APPLIED TO CORNER-FIRED FURNACE

INTRODUCTION

Present day power plants have water-tube furnaces which are large rectangular boxes, with side and height dimensions in proportion to the generating capacity. The walls are made up of parallel tubes carrying the cooling water, and form an enclosure within which fuel and air are injected, mixed and burned at a certain rate.

In the corner-fired furnace four sets of burner banks are placed, one at each corner and directed tangent to a small imaginary circle at the center of the furnace. The streams of fuel and air issuing from each corner impinge on the corresponding one from the adjacent corner. Where these streams meet, intensive turbulence is produced. This action results in the formation of a large vortex with its axis corresponding to the geometric axis of the combustion chamber. As a result of the centrifugal forces, the vortex spreads out and fills the furnace as illustrated in Figures 1 and 2.

The processes that take place inside such a combustion chamber are highly complex in nature and can be classified under three main headings:

    (1)   Fluid dynamics

    (2)   Heat Transfer

    (3)   Chemical Reaction.

The scope of the present study is limited to the first aspect, and more specifically to the fluid dynamics of corner-fired furnaces.

One approach, in the study of flow pattern in furnaces, which has been widely used over the past ten years, is to experiment and carry measurements on small-scale models [1] - [6]. This technique is extremely useful as direct experiments on full scale industrial plants are usually expensive, or too difficult because of large size or high temperatures. However the small-scale model technique has some limitation. For valid extrapolation of the results from the model to the prototype, similarity must exist between them. This implies, among other things, that for each new prototype investigated a new model has to be built.

The ideal approach to this problem is to formulate an analytical theory that rigorously describes the dynamics of the system and check the theory against experiment carried out in a well determined system.

The flow pattern in a corner-fired furnace is rather difficult to describe mathematically and to the best of the author's knowledge, no satisfactory formulation of this system has been presented up to now. This study is an attempt to provide a realistic formulation of the flow phenomenon.

When confronted with the problem of analyzing a large and complex system, the best method of approach is to try to break it into a number of smaller systems having their own characteristics and identity,

and formulate the interrelationship between them. To apply this reasoning to our problem, let us try to visualize the path of a fluid particle from the inlet to the outlet of the system. Right after leaving the burner nozzles, the flow characteristics of the fuel and air stream is very similar to that of a plane-free-jet; when the jet impinges on the rotational vortex in the central zone of the furnace the flow is transformed and developed into a three-dimensional vortex flow which eventually decays while spiralling upwards. Each of these flow configurations: plane-free-jet, vortex and decaying swirl may be represented quite accurately by existing theories.

To describe mathematically the flow pattern in a corner-fired furnace, it is proposed to divide the whole system into three zones. Within each zone the flow pattern would be governed by the theory prevailing in that zone. Values for the variables: velocity and pressure, being continuous function, will be matched at the boundaries between adjacent zones. The three zones, illustrated on Figure 3 are as follows:

(1)   The plane-free-jet zone, with height corresponding to the burner banks, and extending inward from each furnace corner along the burner axis, to the vortex circle inscribed in the square furnace plane area.

(2)   The vortex zone, having the shape of a cylinder with the furnace-side dimension for diameter, and the height of the burner banks.

(3)   <u>The decaying-swirl zone</u>, also cylindrical in shape,
directly above and extending from the vortex zone to the furnace
outlet plane.

OUTLINE OF PRESENT INVESTIGATION

The main object of this investigation is to develop a mathe-
matical model which describes the flow pattern in a system analogous
to that of an isothermal corner-fired furnace.

Given the following input data:

a)   Fluid mass flow

b)   Inlet nozzle width

c)   Inlet nozzle height

d)   Side dimension of square chamber

e)   Angle between nozzle axis and chamber diagonal

The model output are:velocity components and pressure profiles at
different plane perpendicular to chamber longitudinal axis.

To make the model as close as possible to the real system, it
is divided into three zones:

a)   The plane-free jet zone

b)   The vortex zone

c)   The decaying swirl zone.

For each of these three zones, mathematical relationships are derived
for the velocity component and pressure profiles either in closed form
or by numerical approximation. Values of the dependent variables are
matched at the boundary between adjacent zones.

The study is divided into two main parts:

Part 1 - A review of published analytical and experimental works is given and the derivation of mathematical relationships between independent and dependent variables for each of the three zones is formulated.

Part 11 - Results, based on the formulation of Part 1 are given for the domain of interest of the independent parameters. The results are discussed and critically analyzed.

PART 1

THEORETICAL ANALYSIS

1.   THE PLANE-FREE JET ZONE

1.1   REVIEW OF PREVIOUS INVESTIGATIONS

A vast amount of information on the subject of free-jet has been published [7], [8]. Consequently only a brief account of the methods and solutions which are relevant to the present problem will be given.

Free-jet flow may be completely laminar, completely turbulent or transitional (i.e transition from laminar to turbulent flow in the jet). In each of these types of flow the jet may be divided into three separate regions: the potential core surrounded by a mixing zone, the transition zone and the fully developed zone (Figure 4).

The characteristic of jet turbulent motion is that the turbulent fluctuations are random in nature and consequently solution of turbulent flow problem requires the application of statistical methods. G.I. Taylor [9], [10] was the first to develop a statistical theory of turbulence, applicable to continuous movement and satisfying the equation of motion. However, even though it was further developed, this theory deals only with isotropic turbulence which

is the simplest type of turbulence and of very limited use to the solution of practical problem. To overcome these limitations semi-empirical theories, sometimes referred to as phenomenological theories have been developed. The three best known are:

(1) Prandtl's mixing-length theory [11]

(2) Taylor's vorticity theory [12]

(3) Reichardt's inductive theory [13]

Starting with the Navier-Stokes equations, which are obtained by equating the rate of change of momentum of a small volume of fluid to the forces acting on it which consist of a pressure gradient and the force due to internal stresses, Prandtl postulated that this turbulent shear stress was related to the velocity gradient and to the size of the eddy, and that the fluctuating components of velocity were proportional to the mean velocity gradient. In his vorticity theory, Taylor suggested that the turbulent shear stress be determined by the lateral transfer of vorticity rather than by momentum transfer. Reichardt assumed that the transverse transport of momentum is proportional to the transverse gradient of momentum.

The above three theories being semi-empirical, they rely on experiments to establish the needed numerical value of the constants or coefficients. Using Prandtl's mixing-length theory, Tollmien [14] successfully analyzed the problem of turbulent jet mixing of incompressible fluid in a two-dimensional jet issuing from a very narrow opening with a medium at rest. Subsequently, measurements by Ruden [15],

Foerthmann [16] and Kuethe [17] agree fairly well with Tollmien's
results. Gortler [18] re-examined the problem using Reichardt's
assumption with some suggestions from Prandtl [19] and obtained
improvement in the velocity profiles of the jet. More recently
Van der Hegge Zijnen [20] has obtained considerable data on this
particular problem.

1.2   ASSUMED FLOW CONDITIONS

In this investigation, the flow is assumed to be steady,
viscous, isothermal and incompressible. As shown in Figure 4, the
jet may be divided into three separate regions. Region 1 is charac-
terized by a uniform core, shaped roughly in the form of a wedge
tapering from the nozzle width, at the jet source, and vanishing at
a point about 4.5 nozzle widths downstream. The velocity in the core
is uniform provided that the nozzle outlet velocity is uniform.
Surrounding this core is a mixing region where the velocity is not
uniform and varies both axially and transversely. In region II the
velocity profiles continue to develop until they attain a shape which
no longer changes with further increase in distance, thus they are said
to be self-similar. Consequently, region II is a transitional region
in which the velocity profiles adjust from the non self-similar profiles
at the end of region 1 to the self-similar profiles of region III.

The maximum velocity within the jet occurs at the exit of the
nozzle, and the static pressure is constant within the jet structure.
Since there is neither pressure gradient nor wall shear stress in the

free jet, there is no mechanism by which the momentum flux across any transverse section of the jet can be reduced, and we are led to the important conclusion that the total momentum content within the jet is constant. The jet then only spreads the momentum by means of viscous or turbulent mixing.

Our interest is to determine a representative velocity vector at the boundary between the plane-free-jet zone and the vortex zone. It is therefore necessary to establish first a relationship for the length of the free-jet motion so as to determine what velocity profile is to be expected after the jet has travelled this distance.

1.3   DISTANCE OF FREE-JET MOTION

Referring to Figure 5, let the furnace chamber be of square cross section with side 2R, and the nozzle x-axis be inclined with respect to the furnace diagonal by an angle γ . Then by trigonometry the distance d , from the furnace corner (which is coincident with the nozzle plane outlet) to the intersection of nozzle x-axis with the furnace inscribed circle, can be expressed as:

$$d = R \sec \gamma \left(\sqrt{2} - \cos \delta \right) \tag{1}$$

where δ is the angle subtended at the furnace center by a line perpendicular to the furnace diagonal and originating at the intersection point. Table 1 shows calculated values of d for practical values of γ and 2R.

1.4   EQUIVALENT VELOCITY PROFILE

The analysis of the spreading of a plane-free jet involves solutions of the Navier-Stokes momentum equations in conjunction with the continuity equation. In our case of steady, two-dimensional, incompressible and turbulent flow with no pressure gradient, these equations are:

$$\bar{u}\frac{\partial \bar{u}}{\partial x} + \bar{v}\frac{\partial \bar{u}}{\partial y} = \frac{1}{\rho}\frac{\partial \tau_s}{\partial y} \qquad (2)$$

$$\frac{\partial \bar{u}}{\partial x} + \frac{\partial \bar{v}}{\partial y} = 0 \qquad (3)$$

where $\bar{u}$ and $\bar{v}$ are components of velocity in Cartesian coordinates, ρ is the density of the fluid in the jet and τ_s denotes the turbulent shearing stress. Prandtl's mixing-length was derived from the concept that the turbulent shear stress is related to the velocity gradient and to the size of eddy so that:

$$\tau_s = \rho \, \ell^2 \left|\frac{\partial \bar{u}}{\partial y}\right| \frac{\partial \bar{u}}{\partial y} \qquad (4)$$

where ℓ , the mixing length, is dependent on the size of eddy at the relevant point in the jet. Substituting for τ_s in equation (2) from equation (4) we obtain:

$$\bar{u}\frac{\partial \bar{u}}{\partial x} + \bar{v}\frac{\partial \bar{u}}{\partial y} = 2\,\ell^2 \frac{\partial \bar{u}}{\partial y}\frac{\partial^2 \bar{u}}{\partial y^2} \qquad (5)$$

Method of solving these equations is given in standard texts (e.g. [7], [11]). Experiments on this type of jet have been performed by Van der Hegge Zijnen [20] and the following relationships satisfy the data reasonably well in the fully developed region of the jet:

a)   Velocity on the jet axis:

$$\frac{u_m}{V_j} = 2.48 \left(\frac{x}{b} + 0.6 \right)^{-1/2} \tag{6}$$

b)   Transverse profiles of velocity:

$$\frac{\bar{u}}{u_m} = 0.5 \left(1 + \cos \frac{\pi y}{0.192 x} \right) \tag{7}$$

where V_j is the average velocity at nozzle outlet, u_m is the time-mean velocity component on the axis of jet, $\bar{u}$ is the time-mean velocity component parallel to axis of jet and b is the nozzle width.

Substituting for u_m from equation (6) into equation (7), then

$$\bar{u} = 1.24 \, V_j \left(\frac{b}{x + 0.6 \, b} \right)^{1/2} \left(1 + \cos \frac{\pi y}{0.192 \, x} \right) \tag{8}$$

The angle of spread of jets is usually expressed as the jet half-angle, which is the angle subtended at the jet origin by points on the axis and points at which the velocity is half the value on the axis. For the data of Van der Hegge Zijnen the jet half angle was 5.5°. It is included in the velocity profile equation (8) through the constant 0.192 which is equal to 2 tan θ .

However, for the particular problems this study is intended to cover, the range of values for b extends between 1.5 and 2.0 ft. When comparing with the calculated values for d (See Table 1) from equation (1) it is found that $d < 8\,b$. Consequently the jet velocity profile will not be in the fully developed region (i.3 region lll of Figure 4), and the velocity profile, given by equation (8) will not be strictly applicable.

To obtain an average "equivalent" velocity at the boundary between the plane-free jet zone and the vortex zone (i.e when $x = d$) the principle, that for a free-jet the nomentum flux across any transverse section of the jet remains constant, is used. Let the jet lateral boundary line be that of the jet half-angle then,

$$y = \frac{b}{2} + 0.096\,x \qquad (9)$$

At the nozzle outlet the momentum flux $\dot{M}_c$ per unit length of nozzle height is:

$$\dot{M}_c = b\rho\,V_j^2 \qquad (10)$$

At a distance x from the nozzle outlet the momentum flux $\dot{M}_x$ is:

$$\dot{M}_x = 2 \, y \, \rho \, \bar{U}_x^2 \tag{11}$$

where $\bar{U}_x$ is an average velocity at x defined by

$$\bar{U}_x^2 = \int_{-\infty}^{\infty} \bar{u} \, dy$$

Equating equations (11) and (10), then

$$\bar{U}_x = V_j \left(\frac{b}{b + .192 x} \right)^{1/2} \tag{12}$$

At the end of the plane-free jet zone, that is to say when x is equal to d, the average velocity $\bar{U}_d$ is:

$$\bar{U}_d = V_j \left(\frac{b}{b + .192 d} \right)^{1/2} \tag{13}$$

and the equivalent width of the jet W, at the same location is obtained from equation (9),

$$W = b \left(1 + 0.192 \frac{d}{b} \right) \tag{14}$$

2.   THE VORTEX ZONE

2.1   REVIEW OF PREVIOUS INVESTIGATIONS

Since Ranque [21] first mentioned the vortex tube in a French
patent applied for in 1931, many studies, analytical and experimental,
have been undertaken toward the description of flow in a confined vortex.
Typical confined vortex configuration might consist of a cylindrical
chamber with a fluid injected both radially and tangentially at the
chamber periphery and withdrawn at the central axis. This work has
been motivated by interest in a number of devices that utilize such
vortex configuration including the magnetohydrodynamic vortex generator,
the vortex nuclear reactor and recently the vortex amplifier for fluidic
applications. In general, theoretical analyses of vortex flow involve
solutions of the Navier-Stokes equations, but due to the highly non-
linear characteristics of these equations a number of simplifying
assumptions have to be made in order to arrive at some approximate
solutions. Except under certain simple conditions the exact solutions
of the complete Navier-Stokes equations are inacessible.

An extensive review of analytical work on vortex flow has been
given by Donaldson and Sullivan [22], [23]. Sometime later, Lewellen
[24], [25] presented solutions for the cases of a viscous, incompressible
fluid in steady axisymmetric flow with strong or low circulation. More
recently Kwok [26] gave closed-form solutions for confined vortex
incompressible flow within a thin cylindrical chamber.

During the same period, experimental work was carried out by several workers. Donaldson and Snedeker [27] studied the character of vortices in a simple cylindrical vortex chamber having a single end wall rather than the fully confined vortex. Savino and Keshock [28] did careful measurements of radial and tangential velocity components as well as static pressure measurements of a turbulent vortex flow. Subsequently, Roschke [29] investigated a vortex flow of water within a right circular cylinder at different length-to-diameter ratio. Then Kwok [26], to verify his theoretically predicted profiles, measured axial and tangential velocity distributions at the exit plane of the central exhaust orifice, and the radial wall static pressure across the chamber.

2.2   ASSUMED GEOMETRIC CONFIGURATION AND FLOW CONDITIONS

In order to simplify the problem, it is assumed (Figure 6) that the outer boundary of the vortex zone is a cylinder whose diameter is that of a circle inscribed inside a square of side $2R$. The cylinder is closed at the bottom end and open at the top. The height of the zone is that of the inlet nozzle and corresponds to the vertical height of the burner bank in the real system.

As in the preceding zone, the flow is assumed to be steady, viscous, isothermal, turbulent and incompressible. Moreover it is assumed that the flow is axisymmetric with the vortex axis coinciding with the axis of cylindrical coordinate system. Based on the work

of Donaldson and Snedeker [27], and that of Kwok [26] the following

assumptions are made regarding the three-dimensional fluid motion:

(a) $\qquad \bar{v}_r = \bar{v}_r(r)$ $\qquad$ (15)

(b) $\qquad \overline{v}_\phi = \overline{v}_\phi(r)$ $\qquad$ (16)

(c) $\qquad \overline{v}_z = z\, f(r)$ $\qquad$ (17)

Very little is known concerning the turbulent stresses in the case

of the vortex chamber, consequently the approach taken by Kwok [26]

has been retained. It is assumed that the apparent stresses which

are caused by the eddy viscosity ϵ, have a similar influence on

the flow as the viscous stresses, and that the eddy viscosity is

constant throughout the zone.

2.3 EQUATIONS OF MOTION [26]

2.3.1 BASIC EQUATIONS

The Navier-Stokes equations for incompressible turbulent steady

flow in Cartesian coordinates are given in Schlichting [30] p.463 as:

$$\rho\left(\bar{u}\frac{\partial\bar{u}}{\partial x} + \bar{v}\frac{\partial\bar{u}}{\partial y} + \bar{w}\frac{\partial\bar{u}}{\partial z}\right) = -\frac{\partial\bar{p}}{\partial x} + \mu\nabla^2\bar{u} - \rho\left(\frac{\partial\overline{u'^2}}{\partial x} + \frac{\partial\overline{u'v'}}{\partial y} + \frac{\partial\overline{u'w'}}{\partial z}\right) \quad (18a)$$

$$\rho\left(\bar{u}\frac{\partial\bar{v}}{\partial x} + \bar{v}\frac{\partial\bar{v}}{\partial y} + \bar{w}\frac{\partial\bar{v}}{\partial z}\right) = -\frac{\partial\bar{p}}{\partial y} + \mu\nabla^2\bar{v} - \rho\left(\frac{\partial\overline{u'v'}}{\partial x} + \frac{\partial\overline{v'^2}}{\partial y} + \frac{\partial\overline{v'w'}}{\partial z}\right) \quad (18b)$$

$$\rho\left(\bar{u}\frac{\partial\bar{w}}{\partial x} + \bar{v}\frac{\partial\bar{w}}{\partial y} + \bar{w}\frac{\partial\bar{w}}{\partial z}\right) = -\frac{\partial\bar{p}}{\partial z} + \mu\nabla^2\bar{w} - \rho\left(\frac{\partial\overline{u'w'}}{\partial x} + \frac{\partial\overline{v'w'}}{\partial y} + \frac{\partial\overline{w'^2}}{\partial z}\right) \quad (18c)$$

where
$$\nabla^2 = \frac{\partial^2}{\partial x^2} + \frac{\partial^2}{\partial y^2} + \frac{\partial^2}{\partial z^2} \quad (18d)$$

Comparing the set of equations (18) with the set obtained for the laminar case, they are seen to be identical except for additional terms on the right hand side which can be interpreted as components of a stress tensor. Rewriting equation (18) as:

$$\rho\left(\bar{u}\frac{\partial\bar{u}}{\partial x} + \bar{v}\frac{\partial\bar{u}}{\partial y} + \bar{w}\frac{\partial\bar{u}}{\partial z}\right) = -\frac{\partial\bar{p}}{\partial x} + \mu\nabla^2\bar{u} + \left(\frac{\partial\sigma_x}{\partial x} + \frac{\partial\tau_{xy}}{\partial y} + \frac{\partial\tau_{xz}}{\partial z}\right) \quad (19a)$$

$$\rho\left(\bar{u}\frac{\partial\bar{v}}{\partial x} + \bar{v}\frac{\partial\bar{v}}{\partial y} + \bar{w}\frac{\partial\bar{v}}{\partial z}\right) = -\frac{\partial\bar{p}}{\partial y} + \mu\nabla^2\bar{v} + \left(\frac{\partial\tau_{xy}}{\partial x} + \frac{\partial\sigma_y}{\partial y} + \frac{\partial\tau_{yz}}{\partial z}\right) \quad (19b)$$

$$\rho\left(\bar{u}\frac{\partial\bar{w}}{\partial x} + \bar{v}\frac{\partial\bar{w}}{\partial y} + \bar{w}\frac{\partial\bar{w}}{\partial z}\right) = -\frac{\partial\bar{p}}{\partial z} + \mu\nabla^2\bar{w} + \left(\frac{\partial\tau_{zx}}{\partial x} + \frac{\partial\tau_{zy}}{\partial y} + \frac{\partial\sigma_z}{\partial z}\right) \quad (19c)$$

it can be concluded that the components of the mean velocity of turbulent flow satisfy the same equations as those satisfied by laminar flow if the laminar stresses are increased by additional stresses known as apparent or Reynolds stresses.

Assuming that the apparent stresses which are caused by a constant eddy viscosity ϵ have a similar influence on the flow as the viscous stresses, then equation (19) may be written as:

$$\bar{u}\frac{\partial\bar{u}}{\partial x} + \bar{v}\frac{\partial\bar{u}}{\partial y} + \bar{w}\frac{\partial\bar{u}}{\partial z} = -\frac{1}{\rho}\frac{\partial\bar{p}}{\partial x} + \gamma_a \nabla^2\bar{u} \qquad (20a)$$

$$\bar{u}\frac{\partial\bar{v}}{\partial x} + \bar{v}\frac{\partial\bar{v}}{\partial y} + \bar{w}\frac{\partial\bar{v}}{\partial z} = -\frac{1}{\rho}\frac{\partial\bar{p}}{\partial y} + \gamma_a \nabla^2\bar{v} \qquad (20b)$$

$$\bar{u}\frac{\partial\bar{w}}{\partial x} + \bar{v}\frac{\partial\bar{w}}{\partial y} + \bar{w}\frac{\partial\bar{w}}{\partial z} = -\frac{1}{\rho}\frac{\partial\bar{p}}{\partial z} + \gamma_a \nabla^2\bar{w} \qquad (20c)$$

where $\qquad \gamma_a = \dfrac{\mu+\epsilon}{\rho} \qquad\qquad\qquad$ (21)

Changing to cylindrical coordinates r, ϕ, z, with $\bar{v}_r$, $\bar{v}_\phi$, $\bar{v}_z$ as the radial, tangential and axial velocity components then equations (20) becomes:

$$\bar{v}_r\frac{\partial\bar{v}_r}{\partial r} + \frac{\bar{v}_\phi}{r}\frac{\partial\bar{v}_r}{\partial\phi} + \bar{v}_z\frac{\partial\bar{v}_r}{\partial z} - \frac{\bar{v}_\phi^2}{r} = -\frac{1}{\rho}\frac{\partial\bar{p}}{\partial r} + \gamma_a\left(\nabla^2\bar{v}_r - \frac{\bar{v}_r}{r^2} - \frac{2}{r^2}\frac{\partial\bar{v}_\phi}{\partial\phi}\right) \qquad (22a)$$

$$\bar{v}_r\frac{\partial\bar{v}_\phi}{\partial r} + \frac{\bar{v}_\phi}{r}\frac{\partial\bar{v}_\phi}{\partial\phi} + \bar{v}_r\frac{\bar{v}_\phi}{r} + \bar{v}_z\frac{\partial\bar{v}_\phi}{\partial z} = -\frac{1}{\rho r}\frac{\partial\bar{p}}{\partial\phi} + \gamma_a\left(\nabla^2\bar{v}_\phi + \frac{2}{r^2}\frac{\partial\bar{v}_r}{\partial\phi} - \frac{\bar{v}_\phi}{r^2}\right) \qquad (22b)$$

$$\bar{v}_r \frac{\partial \bar{v}_3}{\partial r} + \frac{\bar{v}_\phi}{r}\frac{\partial \bar{v}_3}{\partial \phi} + \bar{v}_3 \frac{\partial \bar{v}_3}{\partial 3} = -\frac{1}{\rho}\frac{\partial \bar{p}}{\partial 3} + \nu_a \left(\nabla^2 \bar{v}_3 \right) \tag{22c}$$

where

$$\nabla^2 = \frac{\partial^2}{\partial r^2} + \frac{1}{r}\frac{\partial}{\partial r} + \frac{1}{r^2}\frac{\partial^2}{\partial \phi^2} + \frac{\partial^2}{\partial 3^2} \tag{22d}$$

and the continuity equation is:

$$\frac{\partial \bar{v}_r}{\partial r} + \frac{\bar{v}_r}{r} + \frac{1}{r}\frac{\partial \bar{v}_\phi}{\partial \phi} + \frac{\partial \bar{v}_3}{\partial 3} = 0 \tag{23}$$

Now making use of the property of axisymmetry (i.e. no dependence on ϕ), and of the assumptions that $\bar{v}_r$ and $\bar{v}_\phi$ are function of r only, then equations (22) and (23) simplify to:

$$\bar{v}_r \frac{d\bar{v}_r}{dr} - \frac{\bar{v}_\phi^2}{r} = -\frac{1}{\rho}\frac{\partial \bar{p}}{\partial r} + \nu_a \left[\frac{d}{dr}\left(\frac{\bar{v}_r}{r} + \frac{d\bar{v}_r}{dr} \right) \right] \tag{24a}$$

$$\bar{v}_r \frac{d\bar{v}_\phi}{dr} + \frac{\bar{v}_r \bar{v}_\phi}{r} = \nu_a \left[\frac{d}{dr}\left(\frac{\bar{v}_\phi}{r} + \frac{d\bar{v}_\phi}{dr} \right) \right] \tag{24b}$$

$$\bar{v}_r \frac{\partial \bar{v}_3}{\partial r} + \bar{v}_3 \frac{\partial \bar{v}_3}{\partial 3} = -\frac{1}{\rho}\frac{\partial \bar{p}}{\partial 3} + \nu_a \left(\frac{\partial^2 \bar{v}_3}{\partial r^2} + \frac{1}{r}\frac{\partial \bar{v}_3}{\partial r} + \frac{\partial^2 \bar{v}_3}{\partial 3^2} \right) \tag{24c}$$

$$\frac{d\bar{v}_r}{dr} + \frac{\bar{v}_r}{r} + \frac{\partial \bar{v}_3}{\partial 3} = 0 \tag{24d}$$

2.3.2 DIMENSIONLESS VARIABLES

To facilitate the solution of the set of equations (24) all
the variables are made dimensionless by comparing the radial and
axial lengths to R , half the furnace side, and comparing the velocity
components and static pressure to the tangential velocity component V
at the inlet of the vortex zone and twice the value of dynamic head ρV^2
respectively. On this basis the dimensionless variables are defined
as:

Length: $\qquad\qquad X = \dfrac{r}{R} \quad , \quad Z = \dfrac{z}{R}$ $\qquad\qquad$ (25a)

Velocity Components: $\quad V_r = \dfrac{\bar{v}_r}{V} \quad , \quad V_\phi = \dfrac{\bar{v}_\phi}{V} \quad , \quad V_z = \dfrac{\bar{v}_z}{V}$ $\quad$ (25b)

Pressure: $\qquad\qquad P = \dfrac{\bar{P}}{\rho V^2}$ $\qquad\qquad\qquad$ (25c)

As in [26] the dimensionless parameter α , β are introduced
and the apparent Reynold number R_e is defined as:

$$\alpha = \frac{Q}{2\pi\, v_a\, h} \qquad , \qquad \beta = -\frac{N\,(bW)^{1/2}}{2\sqrt{2}\,\pi\,R\sin\gamma} \quad , \quad R_e = \frac{VR}{v_a} \qquad (26)$$

where Q is the total fluid flow rate into the zone, N is the number
of inlet nozzles, h is the height of inlet nozzle and W, b and γ
are as previously defined. From equation (26) it can be shown that:

$$R_e = -\frac{\alpha}{\beta} \qquad\qquad (27)$$

Now in terms of the above dimensionless variables the set of equations (24) can be written as:

$$V_r \frac{dV_r}{dX} - \frac{V_\phi^2}{X} = -\frac{\partial P}{\partial X} + \frac{1}{Re}\left[\frac{d}{dx}\left(\frac{V_r}{X} + \frac{dV_r}{dX} \right) \right] \tag{28a}$$

$$V_r \frac{dV_\phi}{dX} + \frac{V_r V_\phi}{X} = \frac{1}{Re}\left[\frac{d}{dx}\left(\frac{V_\phi}{X} + \frac{dV_\phi}{dX} \right) \right] \tag{28b}$$

$$V_r \frac{\partial V_z}{\partial X} + V_z \frac{\partial V_z}{\partial Z} = -\frac{\partial P}{\partial Z} + \frac{1}{Re}\left[\frac{\partial^2 V_z}{\partial X^2} + \frac{1}{X}\frac{\partial V_z}{\partial X} + \frac{\partial^2 V_z}{\partial Z^2} \right] \tag{28c}$$

$$\frac{dV_r}{dX} + \frac{V_r}{X} + \frac{\partial V_z}{\partial Z} = 0 \tag{28d}$$

and equation (17) becomes:

$$V_z = Z\, f(X) \tag{29}$$

2.3.3 BOUNDARY CONDITIONS

To be consistent with the assumption of axisymmetric flow it is required to have a sufficient number of evenly-spaced driving jets at the periphery of the vortex zone. Stated another way: the radial and tangential velocity components should be uniform all around the chamber.

In order to transform the average velocity $\bar{U}_d$, leaving the plane-free jet zone over a width W, into uniform radial and tangential velocity components over a quarter of the periphery of the vortex chamber, we proceed as follows:

Resolving $\bar{U}_d$ into its radial and tangential components and expressing them in terms of the velocity at the nozzle, then:

$$(v_r)_F = V_j \left(\frac{b}{W}\right)^{1/2}\left[\sqrt{2} \cdot \cos \gamma - \frac{d}{R}\right] \tag{30}$$

$$(v_\phi)_F = V_j \left(\frac{b}{W}\right)^{1/2}\left[\sqrt{2} \cdot \sin \gamma \right] \tag{31}$$

where subscript F means: "at the exit of the plane free jet zone".

From the conservation of mass, the total flow through the nozzles must be equal to the radial flow at the periphery of the vortex zone,

consequently

$$Q = V_j \, b \, h \, N = 2\pi R h \, (\bar{v}_r)_V \tag{32}$$

where subscript V means: "at the inlet of the vortex zone".

Let $(\bar{v}_\phi)_V = (v_\phi)_F$

then

$$(\bar{v}_r)_V = \frac{N \, (bW)^{1/2}}{2\pi R \left[\sqrt{2} \cdot \cos\gamma - \frac{d}{R}\right]} \, (v_r)_F \tag{33}$$

and using expression (26) for β

then $(\bar{v}_r)_V = -\beta \dfrac{\sqrt{2} \cdot \sin\gamma}{\left[\sqrt{2} \cdot \cos\gamma - \frac{d}{R}\right]} \, (v_r)_F \tag{34}$

In dimensionless form the boundary conditions in the vortex zone for V_r, V_ϕ and P become:

At X=1: $V_r = \beta$, $V_\phi = 1$, $P = P_0(z)$

At X=0 : $V_r = 0$, $V_\phi = 0$

2.3.4 CLOSED-FORM SOLUTION

As a first-approach to develop the closed-form solution of equations set (28) the Burgers' one-cell vortex solution is selected. In this type of solution, which is applicable to system with low swirl component, resulting in fairly constant axial velocity profile at the exit of the vortex zone, the factor $f(X)$, in the expression for V_z equation (29), is constant.

Then: $$V_z = C_1 Z \tag{35}$$

Using this expression for V_z and substituting in set of equations (28), then

$$V_r \frac{dV_r}{dX} - \frac{V_\phi^2}{X} + \frac{\beta}{\alpha}\left[\frac{d}{dX}\left(\frac{V_r}{X} + \frac{dV_r}{dX}\right)\right] = -\frac{\partial P}{\partial X} \tag{36a}$$

$$V_r \frac{dV_\phi}{dX} + \frac{V_r V_\phi}{X} + \frac{\beta}{\alpha}\left[\frac{d}{dX}\left(\frac{V_\phi}{X} + \frac{dV_\phi}{dX}\right)\right] = 0 \tag{36b}$$

$$C_1 Z = -\frac{\partial P}{\partial Z} \tag{36c}$$

$$\frac{dV_r}{dX} + \frac{V_r}{X} + C_1 = 0 \tag{36d}$$

For convenience let $C_1 = 2k$. The axial velocity becomes

$$V_z = 2 k Z \tag{37}$$

The continuity equation (36d) takes the form

$$\frac{1}{X}\frac{d}{dX}\left(X V_r\right) = -2 k \tag{38}$$

Integrating equation (38) yields

$$V_r = - k X + \frac{A}{X} \tag{39}$$

Now applying the boundary at X=0, then

$$V_r = - k X \tag{40}$$

To obtain the value of k, the conservation of mass is considered, that is to say the total flow Q leaving the vortex zone at $z = h$ must be equal to the total flow at the inlet of the vortex zone through the nozzles. Hence

$$Q = \int_0^r 2\pi r \, \bar{v}_z \, dr \tag{41}$$

In dimensionless form the integration of equation (41) at $Z = \frac{h}{R}$ becomes:

$$\frac{Q}{2\pi R^2 V} = \int_0^1 V_z \, X \, dX = \frac{k \, h}{R} \tag{42}$$

Using the relationship given in equation (26) and (27), then

$$k = - \beta \tag{43}$$

and the axial and radial velocity components take the final form

$$V_z = - 2 \beta Z \tag{44}$$

$$V_r = \beta X \tag{45}$$

The tangential velocity component is obtained by solving equation (36b) which can be expressed as:

$$\frac{1}{R_e}\frac{d^2 V_\phi}{dX^2} + \left[\frac{1}{XR_e} + kX\right]\frac{dV_\phi}{dX} + \left[k - \frac{1}{X^2 R_e}\right] V_\phi = 0 \qquad (46)$$

The above equation is a differential equation with varying coefficients which are a function of the independent variable X. Consequently, this type of system is considered linear in the sense that the principle of superposition applies. The complete solution for V_ϕ is found to be :

$$V_\phi = \frac{A_1}{X} - \frac{A_2}{k R_e X} \, e^{-\frac{k R_e X^2}{2}} \qquad (47)$$

where A_1 and A_2 are constants of integration.

Applying the boundary conditions at $X = 1$ and $X = 0$ and rearranging the solution, equation (47) becomes:

$$V_\phi = \frac{1}{X(1 - e^{-\alpha/2})}\left(1 - e^{-\frac{\alpha}{2}X^2}\right) \qquad (48)$$

The static pressure distribution in the vortex zone is obtained as follows:

$$dP = \frac{\partial P}{\partial z}\,dz + \frac{\partial P}{\partial x}\,dx$$

and

$$P = \int \frac{\partial P}{\partial z}\,dz + \int \frac{\partial P}{\partial x}\,dx \qquad (49)$$

Substituting for $\frac{\partial P}{\partial Z}$ and $\frac{\partial P}{\partial X}$, from equations (36c) and (36a), into equation (49), then combining with equations (40) and (43) and integrating yields:

$$P = \beta z^2 - \beta^2 \left(\frac{X^2}{2} + \frac{2}{\alpha} \right) + \int \frac{V_\phi^2}{X} \, dX + A \qquad (50)$$

where A is a constant of integration.

The value of this constant A is obtained from the boundary condition at $X=1$ and $Z=0$.

Substituting for A in equation (50) and rearranging then

$$P_0 - P = -\beta z^2 + \beta^2 \left(\frac{X^2}{2} - \frac{1}{2} \right) - \int_1^X \frac{V_\phi^2}{X} \, dX = \Delta P \qquad (51)$$

3.   THE DECAYING SWIRL ZONE

3.1   REVIEW OF PREVIOUS INVESTIGATIONS

As for vortex flows, swirling flows have also been the object of a number of analytical and experimental studies. In their investigation of swirl decays in pipe flow Talbot [31] and Collatz & Goertler [32] considered small swirl components superimposed on a fully developed parallel pipe flow. The tangential component of the equation of motion was linearized and the problem reduced to an eigenvalue problem.

Kreith and Sonju [33] made a semi-theoretical analysis of the decay of a turbulent swirl of an incompressible fluid in pipes· For the kinematic eddy viscosi y in the linearized swirl equation they used an empirical expression and obtained, for the turbulent swirl decay, good agreement with experimental data.

Using the complete Navier-Stokes equations, Lavan and Fejer [34] obtained a numerical solution for the laminar swirling flow in the entrance region of pipes. Kinney [35] extended von Karman's similarity hypothesis to a cylindrical geometry and established the condition under which universal velocity similarity will exist for plane-rotating turbulent flow. He derived a universal velocity profile and an eddy viscosity expression from these similarity conditions and evaluated a universal constant in the eddy viscosity equation from Taylor's velocity and wall shear-stress measurements.

Recently Rochino and Lavan [36], using the phenomenological models of the turbulent flow mechanism, studied the problem of incompressible turbulent swirling flow in stationary ducts. They derived the swirl equation from Taylor's modified vorticity transport theory and obtained an eddy viscosity expression from von Karman's similarity hypothesis, for the entire flow field except in a small region close to the wall, where a mixing-length expression analogous to that assumed by Prandtl for parallel flow in channels was used. The theoretical results were compared with the experimental data of Fejer, Lavan and Wolf [37] and agreement between experiment and analysis was satisfactory.

3.2   ASSUMED GEOMETRIC CONFIGURATION AND FLOW CONDITIONS

As for the vortex zone, it is assumed that the outer boundary of the swirling flow is a cylinder whose diameter is that of a circle inscribed inside of a square with side $2R$. The cylinder is open at both ends. Using the same coordinate system as for the vortex zone, the inlet plane of the swirl zone is coincident with the outlet plane of the vortex zone and the origin of the coordinate system for this zone is coincident with the point ($0, \phi, h$) of the vortex zone.

Consistent with the assumptions of the preceding zones the flow is treated as steady, viscous, isothermal, turbulent, axisymmetric and incompressible. However, as in the work of Rochino and Lavan [36] which is summarized in the following section (Section 3.3) , the eddy viscosity is not assumed to be constant, and an expression is derived using von Karman's similarity hypothesis.

3.3 EQUATIONS OF MOTION [36]

3.3.1 BASIC EQUATIONS

The Navier-Stoke equations for steady, incompressible, axisymmetric isothermal flow can be written as:

$$\bar{v}_r \frac{\partial \bar{v}_r}{\partial r} + \bar{v}_z \frac{\partial \bar{v}_r}{\partial z} - \frac{\bar{v}_\phi^2}{r} = -\frac{1}{\rho}\frac{\partial \bar{p}}{\partial r} + \gamma \left[\frac{\partial^2 \bar{v}_r}{\partial r^2} + \frac{1}{r}\frac{\partial \bar{v}_r}{\partial r} + \frac{\partial^2 \bar{v}_r}{\partial z^2} - \frac{\bar{v}_r}{r^2} \right]$$

$$- \left[\frac{\partial (\overline{v_r' v_z'})}{\partial z} + \frac{1}{r}\frac{\partial (r\overline{v_r'^2})}{\partial r} - \frac{\overline{v_\phi'^2}}{2} \right] \tag{52a}$$

$$\bar{v}_z \frac{\partial \bar{v}_\phi}{\partial z} + \bar{v}_r \frac{\partial \bar{v}_\phi}{\partial r} + \frac{\bar{v}_r \bar{v}_\phi}{r} = \gamma \left[\frac{\partial^2 \bar{v}_\phi}{\partial z^2} + \frac{1}{r}\frac{\partial \bar{v}_\phi}{\partial r} + \frac{\partial^2 \bar{v}_\phi}{\partial r^2} - \frac{\bar{v}_\phi}{r^2} \right]$$

$$- \left[\frac{\partial (\overline{v_z' v_\phi'})}{\partial z} + \frac{\partial (\overline{v_r' v_\phi'})}{\partial r} + \frac{2\overline{v_r' v_\phi'}}{r} \right] \tag{52b}$$

$$\bar{v}_z \frac{\partial \bar{v}_z}{\partial z} + \bar{v}_r \frac{\partial \bar{v}_z}{\partial r} = -\frac{1}{\rho}\frac{\partial \bar{p}}{\partial z} + \gamma \left[\frac{\partial^2 \bar{v}_z}{\partial z^2} + \frac{1}{r}\frac{\partial \bar{v}_z}{\partial r} + \frac{\partial^2 \bar{v}_z}{\partial r^2} \right]$$

$$- \left[\frac{\partial (\overline{v_z'^2})}{\partial z} + \frac{1}{r}\frac{\partial}{\partial r}(r\overline{v_r' v_z'}) \right] \tag{52c}$$

where $\gamma = \frac{\mu}{\rho}$,

$$\frac{\partial \bar{v}_z}{\partial z} + \frac{1}{r}\frac{\partial (r\bar{v}_r)}{\partial r} = 0 \tag{52d}$$

Using Taylor's modified vorticity theory, the first three partial differential equations for the radial, tangential and axial velocity components take the following form:

$$\bar{v}_r \frac{\partial \bar{v}_r}{\partial r} + \bar{v}_z \frac{\partial \bar{v}_r}{\partial z} - \frac{\bar{v}_\phi^2}{r} = -\frac{\partial H}{\partial r} + e_{m(r)} \left(\frac{\partial^2 \bar{v}_r}{\partial z^2} - \frac{\partial^2 \bar{v}_z}{\partial r \partial z} \right) \tag{53a}$$

$$\bar{v}_r \frac{\partial \bar{v}_\phi}{\partial r} + \bar{v}_z \frac{\partial \bar{v}_\phi}{\partial z} + \frac{\bar{v}_r \bar{v}_\phi}{r} = e_{m(\phi)} \left(\frac{\partial^2 \bar{v}_\phi}{\partial r^2} + \frac{1}{r} \frac{\partial \bar{v}_\phi}{\partial r} - \frac{\bar{v}_\phi}{r^2} + \frac{\partial^2 \bar{v}_\phi}{\partial z^2} \right) \tag{53b}$$

$$\bar{v}_r \frac{\partial \bar{v}_z}{\partial r} + \bar{v}_z \frac{\partial \bar{v}_z}{\partial z} = -\frac{\partial H}{\partial z} + e_{m(z)} \left(\frac{\partial^2 \bar{v}_z}{\partial r^2} - \frac{1}{r} \frac{\partial \bar{v}_z}{\partial r} - \frac{\partial^2 \bar{v}_r}{\partial r \partial z} + \frac{1}{r} \frac{\partial \bar{v}_r}{\partial z} \right) \tag{53c}$$

where $\quad H = \dfrac{\bar{P}}{\rho} + \dfrac{\overline{v'^2}}{2}$

$$\underline{v}' = \left(v_r' , v_\phi' , v_z' \right)$$

$e_{m(r)} , e_{m(\phi)} , e_{m(z)} \qquad$ = the kinematic eddy viscosity in the radial, tangential and axial directions.

However, in the above equations, the molecular viscosity is neglected following the common assumption of turbulent flow theories

which regard the molecular viscosity as being negligible compared to the eddy viscosity of turbulent flow. This assumption is not valid near a solid boundary. Since it is desired to include such regions in the present investigation the tangential component equation (53b) is modified as follows:

$$\overline{v}_r \frac{\partial \overline{v}_\phi}{\partial r} + \overline{v}_{\overline{\jmath}} \frac{\partial \overline{v}_{\overline{\varsigma}}}{\partial \overline{\jmath}} + \frac{\overline{v_r}\,\overline{v}_\phi}{r} = \left(\mathcal{V} + e_{m(\phi)}\right)\left(\frac{\partial^2 \overline{v}_\phi}{\partial r^2} + \frac{1}{r}\frac{\partial \overline{v}_\phi}{\partial r} - \frac{\overline{v}_\phi}{r^2} + \frac{\partial^2 \overline{v}_\phi}{\partial \overline{\jmath}^2}\right) \qquad (54)$$

3.3.2 DIMENSIONLESS VARIABLES AND ORDER OF MAGNITUDE ANALYSIS

In swirling flow, the axial and tangential velocities are generally prevalent, so that:

$$\overline{v}_r \ll \overline{v}_{\overline{\jmath}} \qquad (55a)$$

$$\overline{v}_r \ll \overline{v}_\phi \qquad (55b)$$

Considering the axial change of $\overline{v}_{\overline{\jmath}}$ it is noted that the axial velocity profile changes only slightly over axial distances since the average value of the axial velocity is a constant. Consequently

$$\frac{\partial \overline{v}_{\overline{\jmath}}}{\partial r} \gg \frac{\partial \overline{v}_{\overline{\jmath}}}{\partial \overline{\jmath}} \qquad (55c)$$

Next the change of $\overline{v}_\phi$ with respect to $\jmath$ is compared to the change of $\overline{v}_{\jmath}$ with respect to $\jmath$. In swirling flow the tangential velocity decreases uniformly to zero whereas the axial velocity is unchanged on the average. Consequently it is thought that:

$$\frac{\partial \overline{v}_\phi}{\partial \jmath} \gg \frac{\partial \overline{v}_{\jmath}}{\partial \jmath} \tag{55d}$$

and hence $\dfrac{\partial \overline{v}_\phi}{\partial \jmath} \gg \overline{v}_r$ since $\overline{v}_r$ is negligible.

Using the set of relationships (55) into equations (53a), (53c), and (54) then:

$$\frac{\partial}{\partial r}\left(\frac{\overline{p}}{\rho} + \frac{\overline{v'}^2}{2}\right) = \frac{\overline{v}_\phi^2}{r} \tag{56a}$$

$$\overline{v}_{\jmath}\frac{\partial \overline{v}_\phi}{\partial \jmath} = \left(\jmath + \epsilon_{m(\phi)}\right)\left(\frac{\partial^2 \overline{v}_\phi}{\partial \jmath^2} + \frac{\partial^2 \overline{v}_\phi}{\partial r^2} + \frac{1}{r}\frac{\partial \overline{v}_\phi}{\partial r} - \frac{\overline{v}_\phi}{r^2}\right) \tag{56b}$$

$$\frac{\partial}{\partial \jmath}\left(\frac{\overline{p}}{\rho} + \frac{\overline{v'}^2}{2}\right) = \left(\jmath + \epsilon_{m(\jmath)}\right)\left(\frac{\partial^2 \overline{v}_{\jmath}}{\partial r^2} - \frac{1}{r}\frac{\partial \overline{v}_{\jmath}}{\partial r}\right) \tag{56c}$$

Equation (56b) is known as the swirl equation and is used to predict the decay of angular momentum in the axial direction.

The swirl equation is non-dimensionalized by using the following dimensionless variables;

$$X = \frac{r}{R} \qquad , \qquad Z = \frac{3}{R} \qquad , E = \frac{\ell \, m(\phi)}{\gamma} \qquad (57a)$$

$$V_r = \frac{\overline{v_r}}{\overline{V_a}} \qquad , \qquad V_\phi = \frac{\overline{v_\phi}}{\overline{V_a}} \qquad , V_z = \frac{\overline{v_3}}{\overline{V_a}} \qquad (57b)$$

where $\overline{V_a}$ is the average axial velocity and is defined as:

$$\overline{V}_a = \frac{Q}{\Pi \, R^2} \qquad (58)$$

and R , γ and Q are as defined previously.

Effecting the transformation, the dimensionless swirl equation becomes:

$$V_z \frac{\partial V_\phi}{\partial Z} = \left(\frac{1+E}{(R_e)_z} \right) \left(\frac{\partial^2 V_\phi}{\partial X^2} + \frac{1}{X} \frac{\partial V_\phi}{\partial X} - \frac{V_\phi}{X^2} + \frac{\partial^2 V_\phi}{\partial Z^2} \right) \qquad (59)$$

where

$$\left(R_e \right)_z = \frac{\overline{V}_a R}{\gamma} \qquad (60)$$

is the axial Reynold's number.

Moreover, as pointed out by Kreith and Sonju [33], one can safely assume that:

$$E \frac{\partial^2 V_\phi}{\partial z^2} \ll V_z \frac{\partial V_\phi}{\partial z} \tag{61}$$

then:

$$V_z \frac{\partial V_\phi}{\partial z} = \left(\frac{1+E}{(Re)_z} \right) \left(\frac{\partial^2 V_\phi}{\partial X^2} + \frac{1}{X} \frac{\partial V_\phi}{\partial X} - \frac{V_\phi}{X^2} \right) \tag{62}$$

The above equation was solved [33] on the basis of the eddy viscosity being a function of the axial Reynold's number. In this analysis, the approach of Rochino and Lavan [36] is followed.

Assuming that the kinematic eddy viscosity for swirling flow is a superposition of that for circular and parallel flows one can write:

$$\ell m = L^2 \left(\frac{\partial V_\phi}{\partial r} - \frac{V_\phi}{r} \right) \tag{63}$$

where L is a length scale in the turbulent flow field. Then using von Karman's similarity theory for cylindrical geometry and turbulent flow, it is shown [36] that the mixing length can be linearly

related to r so that:

$$\varrho_m = K^2 r^2 \left(\frac{\partial \overline{v}_\phi}{\partial r} - \frac{\overline{v}_\phi}{r} \right) \tag{64}$$

where the constant K , based on experimental data is taken as 0.0333.

However, near the wall (i.e $0.9 < X \leq 1$) the length scale has been experimentally verified to be proportional to the distance from it. Hence to satisfy this condition, the eddy viscosity expression in this domain is taken as:

$$\varrho_m = K^2 (1-r)^2 \left(\frac{\partial \overline{v}_\phi}{\partial r} - \frac{\overline{v}_\phi}{r} \right) \tag{65}$$

In dimensionless form, the eddy viscosity expressions are:

$$E = (Re)_z \, K^2 X^2 \left(\frac{\partial V_\phi}{\partial X} - \frac{V_\phi}{X} \right) , \quad 0 \leq X \leq 0.9 \tag{66a}$$

$$E = (Re)_z \, K^2 (1-X)^2 \left(\frac{\partial V_\phi}{\partial X} - \frac{V_\phi}{X} \right), \quad 0.9 < X \leq 1.0 \tag{66b}$$

and are assumed to be always positive.

Substituting the eddy viscosity expressions in the swirl equation (62) yields the following partial differential equation;

$$V_z \frac{\partial V_\phi}{\partial z} = \left(\frac{1}{(R_e)_z} + \left| K^2 \Upsilon \left(\frac{\partial V_\phi}{\partial x} - \frac{V_\phi}{x}\right)\right|\right)\left(\frac{\partial^2 V_\phi}{\partial x^2} + \frac{1}{x}\frac{\partial V_\phi}{\partial x} - \frac{V_\phi}{x^2}\right) \tag{67}$$

where $\Upsilon = X^2$ for $0 \leq X \leq 0.9$

$\Upsilon = (1-X)^2$ for $0.9 < X \leq 1.0$

and with the boundary conditions:

(a) $V_\phi(1,z) = 0$

(b) $V_\phi(X,0) = f(x)$

(c) $V_\phi(0,z) = 0$

3.3.3 NUMERICAL SOLUTION

Equation (67) is a highly non-linear partial differential equation of the parabolic type, and consequently a numerical solution method has been selected in preference to a closed form solution attempt.

For convenience, equation (67) is transformed in terms of the angular momentum of the fluid. Let

$$\Gamma = X V_\phi \tag{68}$$

and substituting into equation (67), we obtain:

$$\frac{\partial \Gamma}{\partial z} = \frac{1}{V_z}\left(\frac{1}{(R_e)_z} + \left| \frac{K^2 \Upsilon}{X}\left(\frac{\partial \Gamma}{\partial x} - \frac{2\Gamma}{X}\right)\right|\right)\left(\frac{\partial^2 \Gamma}{\partial x^2} - \frac{1}{X}\frac{\partial \Gamma}{\partial x}\right) \tag{69}$$

with the corresponding boundary conditions:

(a) $\Gamma(1,z) = 0$

(b) $\Gamma(x,0) = X f(x)$

(c) $\Gamma(0,z) = 0$

If we let:

$$D = \frac{1}{V_z} \left(\frac{1}{(Re)_z} + \left| \frac{K^2 r}{X} \left(\frac{\partial \Gamma}{\partial X} - \frac{2\Gamma}{X} \right) \right| \right) \tag{70}$$

Then the angular momentum equation (69) takes the following form:

$$\frac{\partial \Gamma}{\partial z} = D \frac{\partial^2 \Gamma}{\partial X^2} - \frac{D}{X} \frac{\partial \Gamma}{\partial X} \tag{71}$$

To solve equation (71) numerically it is necessary to replace it by a system of finite difference equations. The second order derivative is replaced by three point central differences, and for the first order derivatives, forward differences are used. Figure 7 shows the grid notation for the numerical scheme.

Let

$$\Gamma_i^j = \Gamma(i \Delta x, j \Delta z)$$

then

$$\frac{\partial \Gamma}{\partial z} = \frac{\Gamma_i^{j+1} - \Gamma_i^j}{\Delta z}$$

$$\frac{\partial \Gamma}{\partial X} = \frac{\Gamma_{i+1}^{j} - \Gamma_{i}^{j}}{\Delta X}$$

$$\frac{\partial^2 \Gamma}{\partial X^2} = \frac{\Gamma_{i+1}^{j} - 2\Gamma_{i}^{j} + \Gamma_{i-1}^{j}}{(\Delta X)^2}$$

and substituting into equation (71) we obtain:

$$\Gamma_{i}^{j+1} = \left(\frac{1}{(\Delta X)^2} - \frac{1}{(\Delta X)X_i}\right) D \cdot \Delta Z \, \Gamma_{i+1}^{j} + \left(1 - \left(\frac{2}{(\Delta X)^2} - \frac{1}{(\Delta X)X_i}\right) D \cdot \Delta Z\right) \Gamma_{i}^{j}$$

$$+ \frac{D \cdot \Delta Z}{(\Delta X)^2} \Gamma_{i-1}^{j} \tag{72}$$

where

$$D = \frac{1}{V_z}\left(\frac{1}{(Re)_z} + \left| K^2 X_i \left(\frac{\Gamma_{i+1}^{j} - \Gamma_{i}^{j}}{\Delta X} - \frac{2\Gamma_{i}^{j}}{X_i}\right)\right|\right), \quad 0 \le X \le 0.9$$

$$D = \frac{1}{V_z}\left(\frac{1}{(Re)_z} + \left| K^2 \frac{(1-X_i)^2}{X_i}\left(\frac{\Gamma_{i+1}^{j} - \Gamma_{i}^{j}}{\Delta X} - \frac{2\Gamma_{i}^{j}}{X_i}\right)\right|\right), \quad 0.9 < X \le 1.0$$

Equation (72) is an explicit positive type-difference equation if the following inequalities are satisified:

$$\left(\frac{1}{(\Delta X)^2} - \frac{1}{(\Delta X)X_i}\right) D \cdot \Delta Z \ge 0$$

and $\qquad \left(\dfrac{2}{(\Delta x)^2} - \dfrac{1}{x_i \, (\Delta x)} \right) D \cdot \Delta z \;\; \leq \;\; 1.0$

It can be shown [36] that the above inequalities are always satisified in the present study.

A required input to this numerical scheme is the tangential velocity at the inlet (i.e. $Z = 0$), which is provided by the tangential velocity distribution from the outlet of the vortex zone. The axial velocity profile which appears as a parameter in equation (72) is evaluated by taking the mean between the axial velocity profile at the outlet of the vortex zone and $\overline{V_a}$.

The stepwise integration of the explicit finite difference equation was carried out on an IBM-360 digital computer. Twenty subdivisions were used in the radial direction, and the ratio of Δz to Δx was kept at 0.2.

PART II

THEORETICAL RESULTS

1.   INTRODUCTION

From the sets of solutions, either in closed-form or in
differential form, developed in Part 1, it can be seen that, given
the chamber and nozzles geometries and the properties and flow rate of
the fluid, velocity component profiles and pressure difference distributions
can be calculated in the vortex zone. Also the decay of the tangential
velocity component, as the fluid travels through the subsequent zone
can be obtained. However, in the vortex zone it is necessary to
know the proper value for the apparent kinematic viscosity ν_a
which is a characteristic of the system. In the following theoretical
results the eddy viscosity has been assumed to be 100 fold greater
than the molecular viscosity.

The theoretical results presented in this section are based
on the following values of the independent parameters:

Side dimension of square
chamber, (2R)   :   30', 35', 40'

Angle between nozzle axis
and chamber diagonal, (γ) :   3°, 6°, 9°

Inlet nozzle width, (b)   : 1.666', 1.833', 2'

Inlet nozzle height, (h)   :   33',   30', 27.5'

Fluid Mass flow   : 2,200,000 lbs/hr.

Fluid properties:

    a) density, (ρ):   0.00155 slug/ft^3

    b) Molecular viscosity, (μ): 1.66 x 10^{-5} slug/sec.ft.

Numerical computation of the velocity profiles and pressure distribution of the eighty-one possible combinations of the independent parameters were carried out on an IBM 360 computer.

When grouped into the dimensionless parameters α and β, these combinations of the independent parameters resulted into twenty seven values for β and three values for α in the following domain:

$$55 \leqslant \alpha \leqslant 66$$
$$-1.45 \leqslant \beta \leqslant -0.34$$

2.   RESULTS AND DISCUSSIONS

2.1   THE PLANE-FREE JET ZONE

In this zone it is of interest to know how the resolved components of the average equivalent velocity vector $\bar{U}_d$ do vary with the physical parameters R, b, and γ. Figures 8 and 9 depict graphically equations (30) and (31) respectively. From these figures it is apparent that the ratio of the radial component to the nozzle velocity varies little with any change in the three parameters. This can be explained quite simply as follows:

-44-

1)   The b-dependence is absorbed in the ratio through the nozzle velocity Vj which is inversely dependent on b.

2)   The value of the ratio Vr/Vj is mainly determined by the cosine of γ which, for the low values of γ used, does not vary appreciably.

3)   Similarly, the R-dependence is through the d/R ratio which is proportional to the secant of γ, an almost constant value in the range of γ values used here.

The observed strong dependence on γ of the ratio of the tangential component to the nozzle velocity, is the result of the change in the sine function for the low values of γ.

Figure 10 shows the functional relationship of the radial velocity component from the outlet of the Plane-Free Jet Zone to the inlet of the Vortex Zone. It is the graphical representation of equation (33), with equations (1) and (14) substituted for d and W. The function is seen to be decreasing with b decreasing and R increasing. It does not vary appreciably with γ due to the counteracting influence of β-and sine of γ functions and consequently the plot is shown for one value of γ only. As mentioned previously, this function results from transforming the average equivalent velocity $\bar{U}_d$, leaving the Plane-Free Jet Zone over a width W, into uniform radial and tangential velocity components acting over a quarter of the periphery of the vortex zone.

2.2   THE VORTEX ZONE

Before presenting the dimensionless velocity profiles for
this zone it is of interest to discuss the two dimensionless para-
meters α and β and their relationship with the independent physical
parameters of the system.

When the defining equation (26) is combined with equation (32),
the parameter α is seen to be a Reynold's number, $\frac{R(\overline{v}r)v}{\gamma a}$, based on the
radial velocity component at the inlet of the vortex zone and the
apparent kinematic viscosity.   The dimensionless parameter β on the
other hand, is a grouping of the physical independent parameters:
γ , R, and b.   Its functional dependence on γ for several values of
R and fixed value of b is shown on Figure 11.   It is apparent that β
is mainly dependent on γ in the low range of $\gamma < 8°$ and to a lesser
extent on R while the dependence on b is very small.   The physical
meaning of the β parameter is that it represents the ratio of the
radial to the tangential velocity component at the inlet of the Vortex
Zone.

The dimensionless tangential velocity distribution is shown
on Figure 12 for the three values of α .   It is seen from this figure
that the value of the maximum velocity is increasing and the point
at which it occurs moves closer toward the center as the value of α
is increased.   Remembering that the α parameter, a Reynold's number, is
directly proportional to the chamber geometry and the inlet radial
velocity component and inversely proportional to the apparent kinematic
viscosity, it is seen that the tangential velocity profile shows a

strong tendency, as the absolute value of this Reynold's number
is made larger, for the fluid to conserve its initial angular momentum.

The dimensionless radial and axial velocity profiles are shown
on Figures 13 & 14 respectively. The direct dependence on the
parameter β for both profiles and the proportional dependence on X
for the radial velocity are evident.

The pressure difference distribution is plotted on Figure 15.
The dependence on Z has been removed by making the Z-term in equation
(51) equal to zero. The other two terms in this equation account for
the decelaration of the radial flow and the balancing of the
centrifugal forces. As in the case of the tangential velocity
distribution the dependence on the parameter α is clearly shown
indicating the influence o᷵ the chamber geometry, the inlet radial
velocity component and the apparent kinematic viscosity.

2.3   THE DECAYING SWIRL ZONE

For this zone, dimensionless tangential velocity distributions
are shown on Figures 16, 17 and 18. The three sets of distributions
are for different systems characterized by a different α value but
having a common β value. For each set, two curves are shown: one
corresponding to $\gamma/R = 0$ and the second to $\gamma/R = 9$. When comparing
these graphs two things can be noted:

1)   For increasing α , the relative decrease in the
maximum velocity, i.e. $\left[(V_\phi)_{\substack{Max. \\ Z=0}} - (V_\phi)_{\substack{Max \\ Z=9}} \right] \Big/ \left(V_\phi \right)_{\substack{Max. \\ Z=0}}$,   is
increasing.

2) The point of maximum velocity moves radially inward as the axial distance increases.

It is also apparent that the angular momentum decays with increasing axial distance. As the flow proceeds downstream, the outer region first approaches an irrotational behavior, particularly in the region near the outer boundary. This irrotational flow field widens and progresses toward the axis of the chamber.

CONCLUSION

A mathematical model describing the flow pattern in systems similar to corner-fired furnace, with fluid having constant physical properties, has been proposed.

The approach taken to solve this problem has been to divide the whole system into three zones: the plane-free-jet zone, the vortex zone and the decaying-swirl zone. For each zone the appropriate theory describing the flow pattern is selected and the output variables of one zone are used as input variables in the following zone.

In the theoretical analysis section, development of solutions for the velocity components and pressure difference distribution are given either in closed-form or in difference-equation form. Starting with the plane-free jet zone it is shown that the flow does not become fully developed before reaching the vortex zone and consequently an expression for an equivalent velocity is derived using the principle of momentum flux conservation. In the vortex zone the Burger's one-cell solution, in which the radial and tangential velocities are a function of radius only while the axial velocity is a function of the axial coordinate, has been selected. The independent parameters of the system and the apparent kinematic viscosity, which is assumed constant in this zone, are grouped into two dimensionless numbers: α and β, and the solution to the dimensionless velocity components are expressed as function of these two parameters. In the decaying-swirl zone, the swirl equation is deduced from Taylors' modified vorticity transport theory using an eddy viscosity expression based on an extension of

Von Karman's similarity hypothesis to a cylindrical geometry with a fully turbulent swirling flow. For the region near the wall appropriate modification in the swirl and eddy viscosity expression were made.

Numerical results from the mathematical model were computed and expressed in graphical form showing the effect of the independent parameters on the flow pattern of the system.

RECOMMENDATION FOR FUTURE STUDIES

The mathematical model presented in this study is thought to be an adequate tool to obtain the flow pattern in system similar to the corner-fired furnace. However, it is evident that assurance of this adequacy can be ascertained only by carrying out measurements on real systems, having configuration and dimensions comparable to those for which the mathematical model is felt to be applicable. It is therefore recommended that such testing be implemented and the experimental results compared with the theoretical one.

In order to simplify the complex mathematics involved in solving the Navier-Stokes equations in the vortex zone, a constant apparent viscosity γa is assumed throughout this zone. However, it has been reported [37] that eddy viscosity in swirling flow is a strong function of radial position and a weak function of axial position. An obvious extension of the present study would be to consider the apparent viscosity as a function of r and obtain the solutions to the velocity component profiles with this added refinement.

As a first-approach to develop the closed-form solution of the vortex zone equations, the Burger's one-cell vortex solution was used in the present study. This vortex structure is applicable to system with low swirl component, but as the ratio of the tangential to radial velocity component is increased beyond a certain value a two-cell vortex structure developes. Donaldson and Snedeker [27] experimentally found this critical ratio for the transition from one-cell to two-cell

vortex structure to be approximately 3, which is equivalent in our notation to a β of -.333. Although the cylindrical vortex chamber they used was different, in a number of aspects, from the system of the present study, making their results not directly applicable, it would be useful to consider a two-cell vortex solution so as to extend the range of application of the model.

In addition, to continue the improvement of the present model, it is recommended that extensions to the existing solutions should be made to include the energy generation aspect of the problem and the corresponding volumetric change taking place in such system.

REFERENCES

[1]   Evans, D.G., Patrick, M.A.
            "The Use of Modelling Studies in Boiler Furnaces
            Investigations"
            Journal of the Institute of Fuel, October 1966,
            pages 414 - 421

[2]   Patterson, R.C., Abrahamsen, R.F.
            "Flow Modelling of Furnaces and Ducts"
            ASME Trans. Journal of Engineering for Power, October 1962,
            pages 345 - 357

[3]   Curtis, R.W., Johnston, L.E.
            "Use of Flow Models for Boiler-Furnace Design"
            ASME Trans., Journal of Engineering for Power, October 1959,
            pages 371 - 379

[4]   Chesters, J.H.
            "The Aerodynamic Approach to Furnace Design"
            ASME Trans., Journal of Engineering for Power, October 1959,
            pages 361 - 370

[5]   Putnam, A.A., Ungar, E.W.,
            "Basic Principles of Combustion-Model Research"
            ASME Trans., Journal of Engineering for Power, October 1959,
            pages 383 - 388

[6]   Zelkowski, J.
            "Die isothermische modellierung der strömung in
            Brennkammern von staubkesseln mit eckenbrennern"
            Mitteilungen der VGB, Heft 104, Oktober 1966

[7]   Pai, S.J.
            "Fluid Dynamics of Jets"
            D. Van Nostrand Company, Inc., 1954

[8]   Abramovich, G.N.
            "The Theory of Turbulent Jets" (Translation by Scripta
            Technica, Ed.: L.H. Schindel) M.I.T. Press, Cambridge,
            Mass. 1963

[9]   Taylor, G.I.
        "Diffusion by Continuous Movements"
        Proc. London Math. Soc. 20, page 196, 1920

[10]   Taylor, G.I.
        "Statistical Theory of Turbulence" 1 to V
        Proc. Roy. Soc. (London), A 151, page 135 (1935)
        page 156, 307 (1936)

[11]   Goldstein, S.
        "Modern Developments in Fluid Dynamics"
        Oxford University Press, 1938

[12]   Taylor, G.I.
        "The Transport of Vorticity and Heat Through Fluid in
        Turbulent Motion"
        Proc. Roy. Soc. (London) A-135, pages 685 - 705, 1932

[13]   Reichardt, H.
        "Über ein neue theorie der freien Turbulenz"
        ZAMM, Bd. 21, Nr. 5, pages 257 - 264, 1941
        also Jour. of Roy. Aero. Soc. pages 167 - 176, June 1943

[14]   Tollmien, W.
        "Berechnung der Turbulenten Ausbreitungsvorgänge"
        ZAMM, Bd. IV, page 468, 1926
        also NACA-TM-1085, 1945

[15]   Ruden, P.
        "Turbulente ausbreitung im freistrohl"
        Die Naturwissenschaften, 21 pages 375 - 378, 1933

[16]   Förthmann, E.
        "Über Turbulente Strahlausbreitung"
        Ing, Arch. Bd. V, page 42, 1934
        also NACA-TM-789, 1936

[17]   Kuethe, A.M.
        "Investigations of the Turbulent Mixing Regions Formed
        by Jets"
        Journal of Applied Mechanics, 2, No. 3, pages A-87 - 95,
        1935

[18]   Görtler, H.
         "Berechnung von aufgaben der freien turbulenz auf grund
         neuen Naherungsansatzes"
         ZAMM, Vd. 22, Nr. 5, pages 244 - 254, 1942

[19]   Prandtl, L.
         "Bemerkungen zur theorie der freien turbulenz"
         ZAMM, Bd. 22, Nr. 5, pages 241 - 243, 1942

[20]   Van der Hegge Zignen, B.G.
         "Measurements of the Velocity Distribution in a Plane
         Turbulent Jet of Air"
         Applied Science Research, A.7, pages 256 - 313, 1958

[21]   Ranque, G.J.
         "Expérience sur la détente giratoire avec productions
         simultanées d'un échappement d'air chaud et d'un
         échappement d'air froid"
         Journal de Physique et le Radium, Tome IV, Série VII
         page 112, 1933
         Bulletin Bi-Mensuel, S-115, 1933

[22]   Donaldson, C. du P., Sullivan, R.D.
         "Examination of the Solutions of the Navier-Stokes
         Equations for a Class of Three-Dimensional Vortices"
         Aero Research Associates of Princeton, AFOSR, TN 60-1277
         1960

[23]   Donaldson, C. du P., Sullivan, R.D.
         "Behaviour of Solutions of the Navier-Stokes Equations
         for a Complete Class of Three-Dimensional Viscous
         Vortices"
         Proc. of the Heat Transfer and Fluid Mechanics Institute
         Stanford University, 1960

[24]   Lewellen, W.S.
         "A Solution for Three-Dimensional Vortex Flows with Strong
         Circulation"
         Journal of Fluid Mechanics, Vol. 14, pt. 3, pages 420 - 432
         1962

[25]   Lewellen, W.S.
         "Linearized Vortex Flows"
         AIAA Journal, Vol. 3, No. 2, pages 91 - 98, 1965

[26]   Kwok, C.K.K.
        "Vortex Flow in a Thin Cylindrical Chamber and Its
        Application in Fluid Amplifier Technology"
        Ph.D. Thesis, McGill University, Montreal, 1966

[27]   Donaldson, C. du P., Snedeker, R.S.
        "Experimental Investigation of the Structure of Vortices
        in Simple Cylindrical Vortex Chambers"
        Aeron. Res. Assoc. of Princeton Inc. Rept. No. 47, 1962

[28]   Savino, J.M., Keshock, E.G.
        "Experimental Profiles of Velocity Components and Radial
        Pressure Distribution in a Vortex Contained in a Short
        Cylindrical Chamber"
        NASA TN D-3072, 1965

[29]   Roschke, E.G.
        "Experimental Investigations of a Confined Jet-Driven
        Water-Vortex"
        NASA Rept. No. 32-982, 1966

[30]   Schichting, H.
        "Boundary Layer Theory", 4th edition
        McGraw Hill Book Company, 1960

[31]   Talbot, L.
        "Laminar Swirling Pipe Flow"
        Journal of Applied Mechanics, Vol. 21, pages 1 - 7,
        1954

[32]   Collatz, L., Görtler, H.
        "Rohrströmung mit schwachem Drall"
        ZAMM 5, pages 95 - 110, 1954

[33]   Kreith, F., Sonju, O.
        "The Decay of Turbulent Swirl in a Pipe"
        Journal of Fluid Mechanics, Vol. 22, part 2, page 257,
        1965

[34]   Lavan, Z., Fejer, A.A.
        "Investigation of Swirling Flows in Ducts"
        IIT Research Institute, ARL 66-0083, 1966

[35]   Kinney, R.B.
         "Universal Velocity Similarity in Fully Turbulent
         Rotating Flows"
         ASME Transactions, Journal of Applied Mechanics,
         pages 437 - 442, 1967

[36]   Rochino, A., Lavan, Z.
         "Analytical Investigations of Incompressible Turbulent
         Swirling Flow in Stationary Ducts"
         ASME Transactions, Journal of Applied Mechanics,
         pages 151 - 158, 1969

[37]   Fejer, A., Lavan, Z., Wolf, L.
         "Study of Swirling Fluid Flows"
         Aerospace Research Laboratories, ARL 68-0173, 1968

TABLE 1 - <u>LENGTH OF FREE-JET MOTION</u> (ft.)

γ	$2R$ (ft.)					
(°)	15	20	25	30	35	40
1	3.10722	4.14296	5.17870	6.21444	7.25018	8.28593
2	3.11047	4.14730	5.18412	6.22095	7.25777	8.29460
3	3.11258	4.15010	5.18763	6.22515	7.26268	8.30020
4	3.11661	4.15550	5.19438	6.23325	7.27213	8.31230
5	3.12318	4.16424	5.20530	6.24636	7.28742	8.32848
6	3.13021	4.17361	5.21701	6.26042	7.30382	8.34722
7	3.13904	4.18539	5.23174	6.27809	7.32443	8.35707
8	3.15752	4.21002	5.26253	6.31503	7.36754	8.42004
9	3.16048	4.21397	5.26746	6.32096	7.37445	8.42794
10	3.17236	4.22981	5.28726	6.34472	7.40217	8.45962
11	3.18589	4.24785	5.30981	6.37177	7.43374	8.49570
12	3.20066	4.26755	5.33444	6.40133	7.46821	8.53510
13	3.21663	4.28884	5.36105	6.43326	7.50547	8.57768
14	3.23378	4.31170	5.38963	6.46755	7.54548	8.62340
15	3.25193	4.33591	5.41989	6.50387	7.58784	8.67182
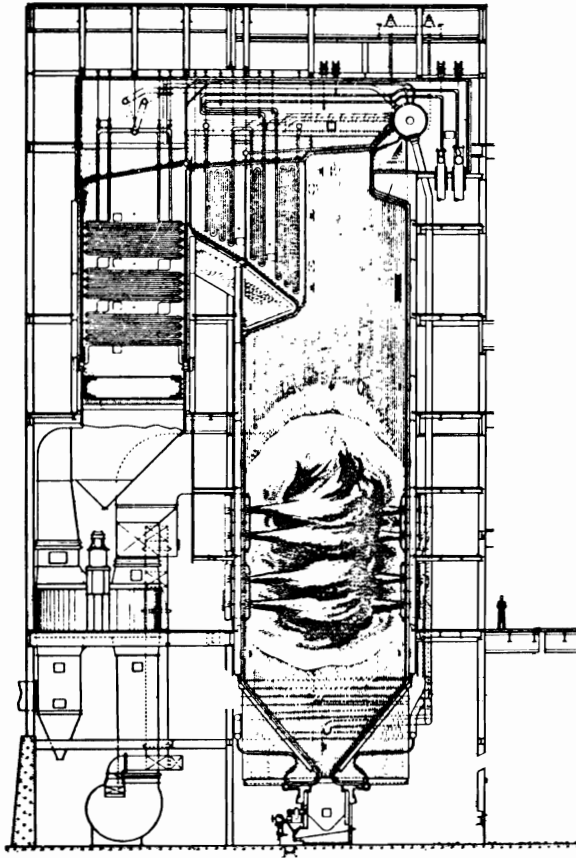
FIGURE 1   CORNER-FIRED FURNACE
(SIDE ELEVATION)
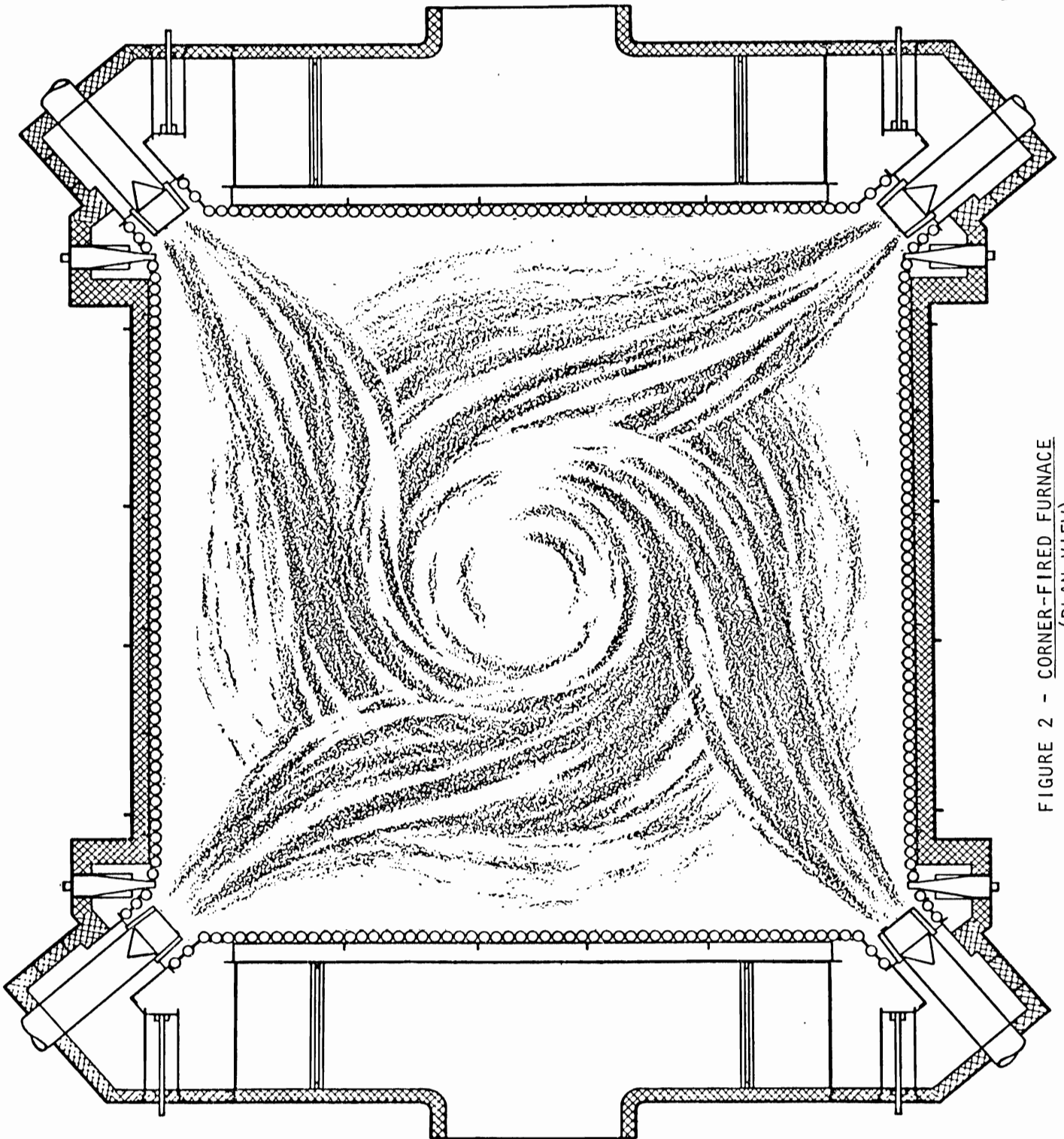
FIGURE 2 - CORNER-FIRED FURNACE
(PLAN VIEW)

Decaying-Swirl
Zone

Vortex Zone

----- Boundaries of Real System
_____ Boundaries of Model
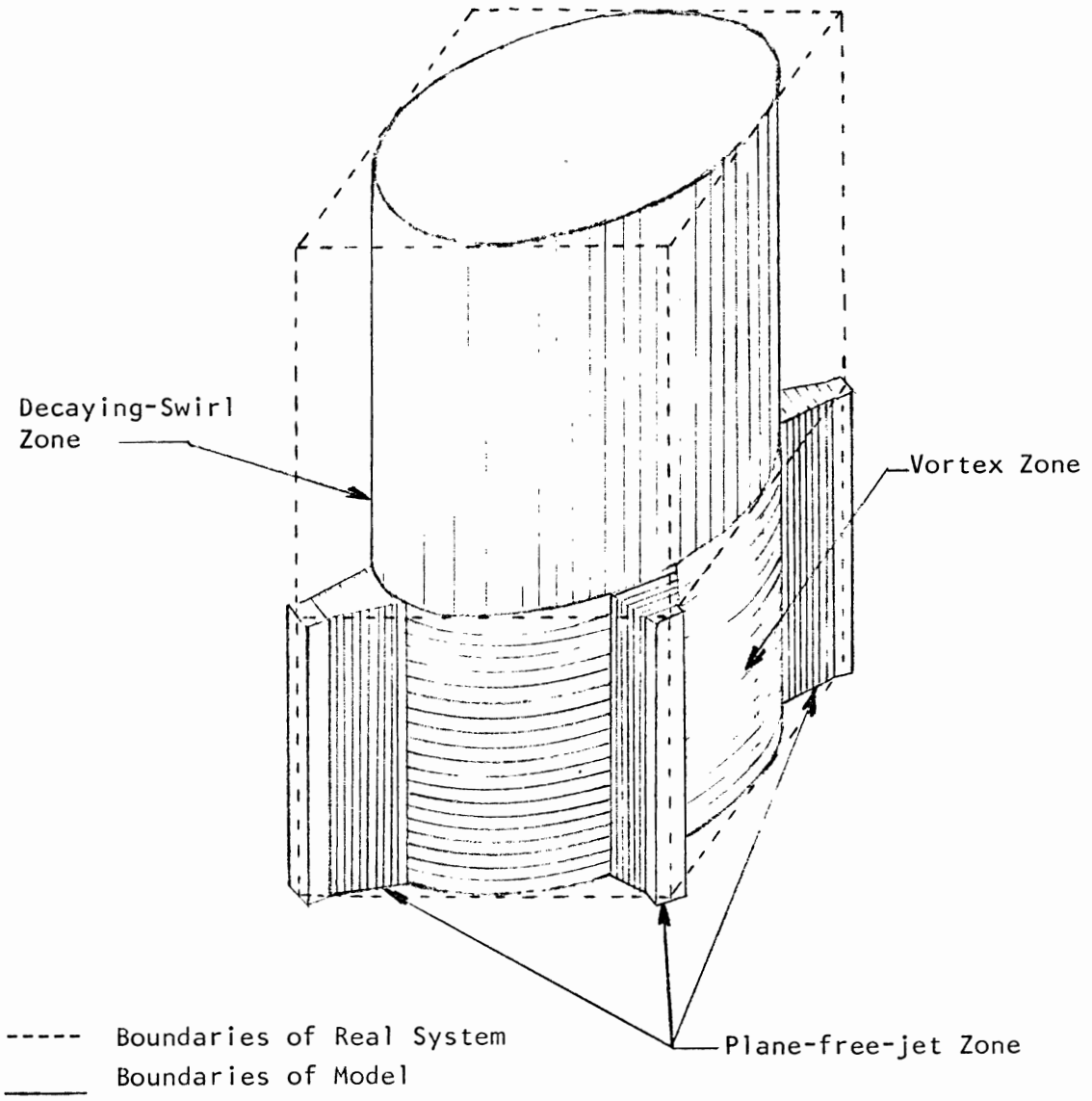
Plane-free-jet Zone

FIGURE 3 - THE THREE-ZONES MODEL
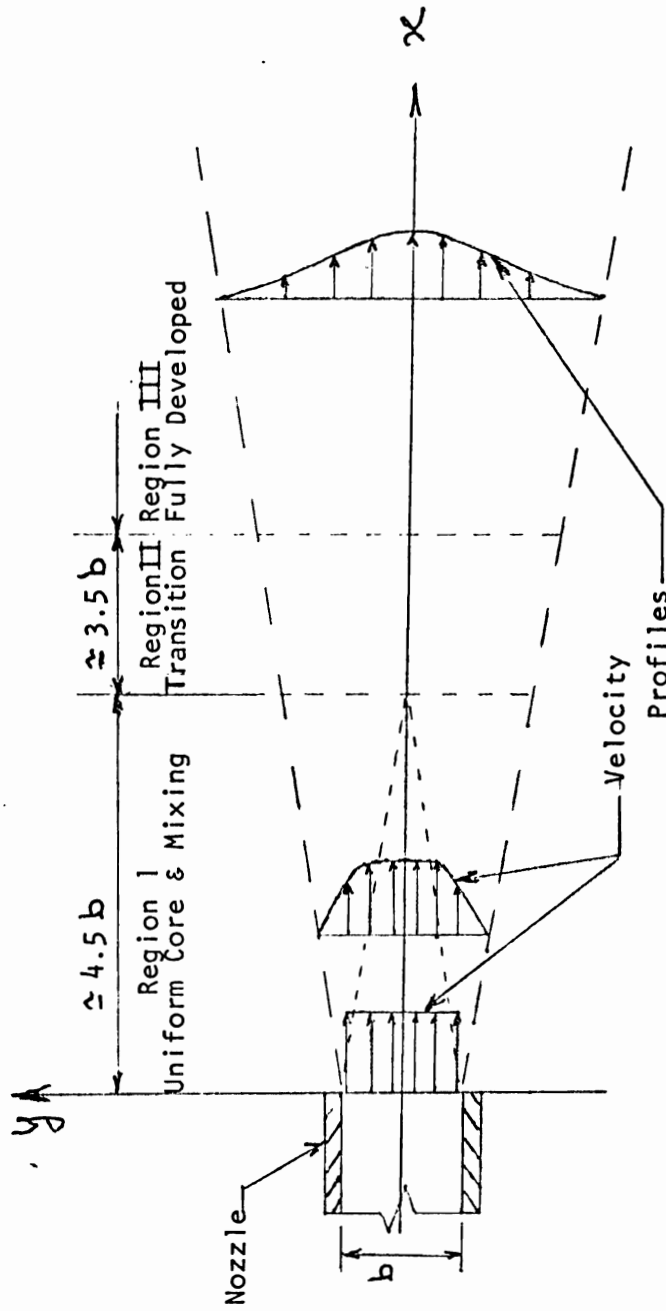
FIGURE 4 — PLANE-FREE-JET (turbulent)
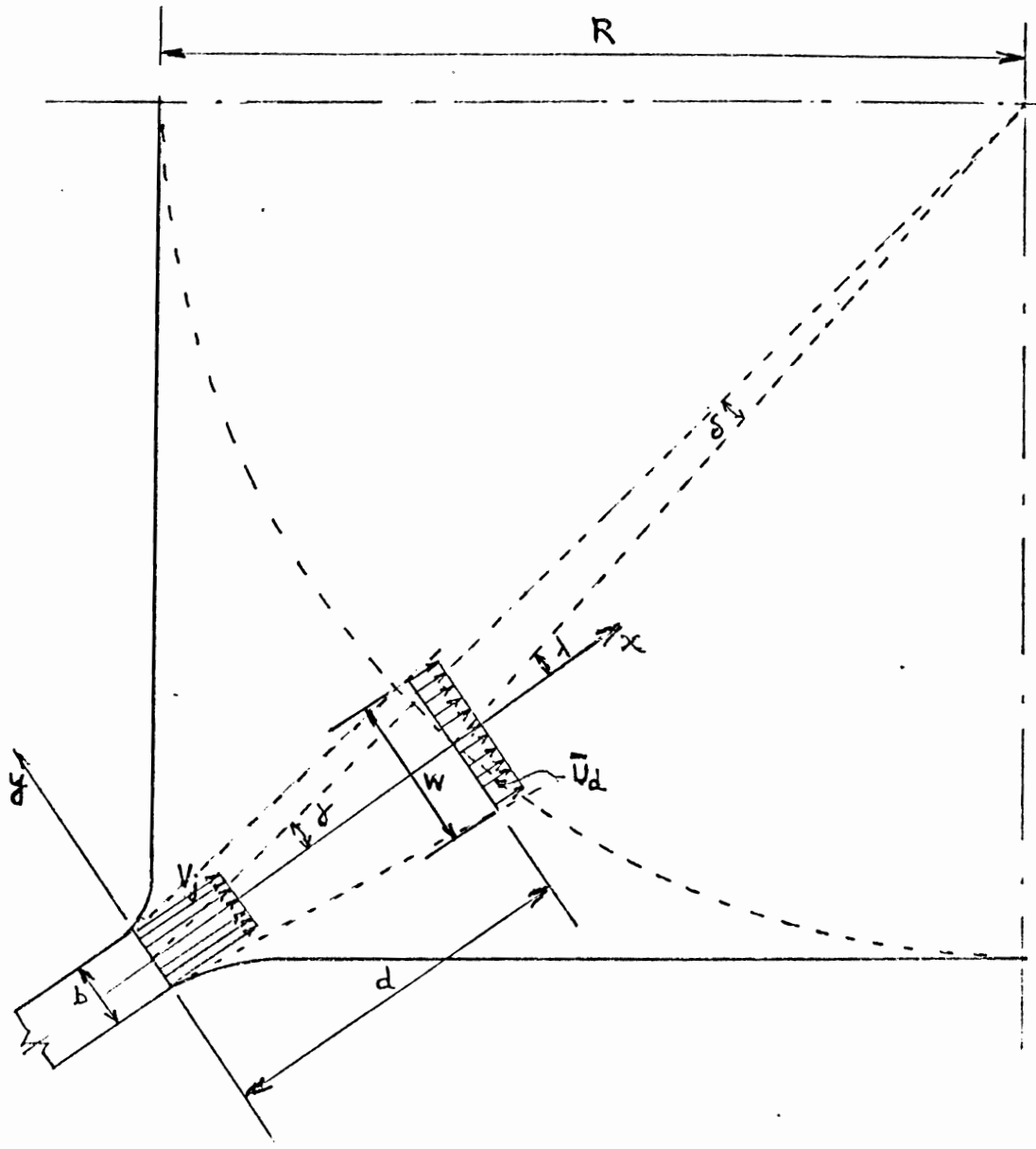
FIGURE 5 - PLANE-FREE-JET ZONE
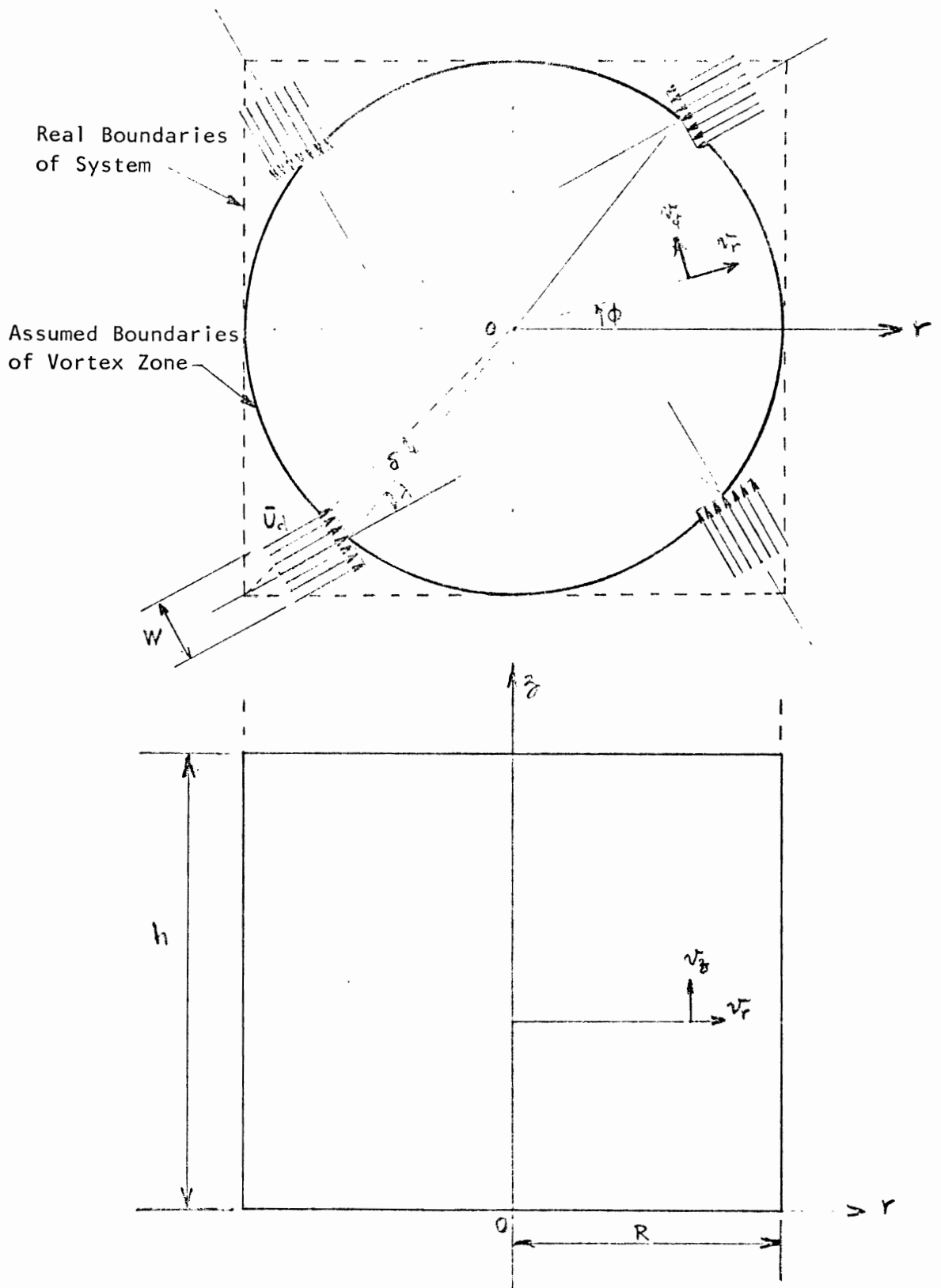
FIGURE 6 - <u>VORTEX ZONE</u>
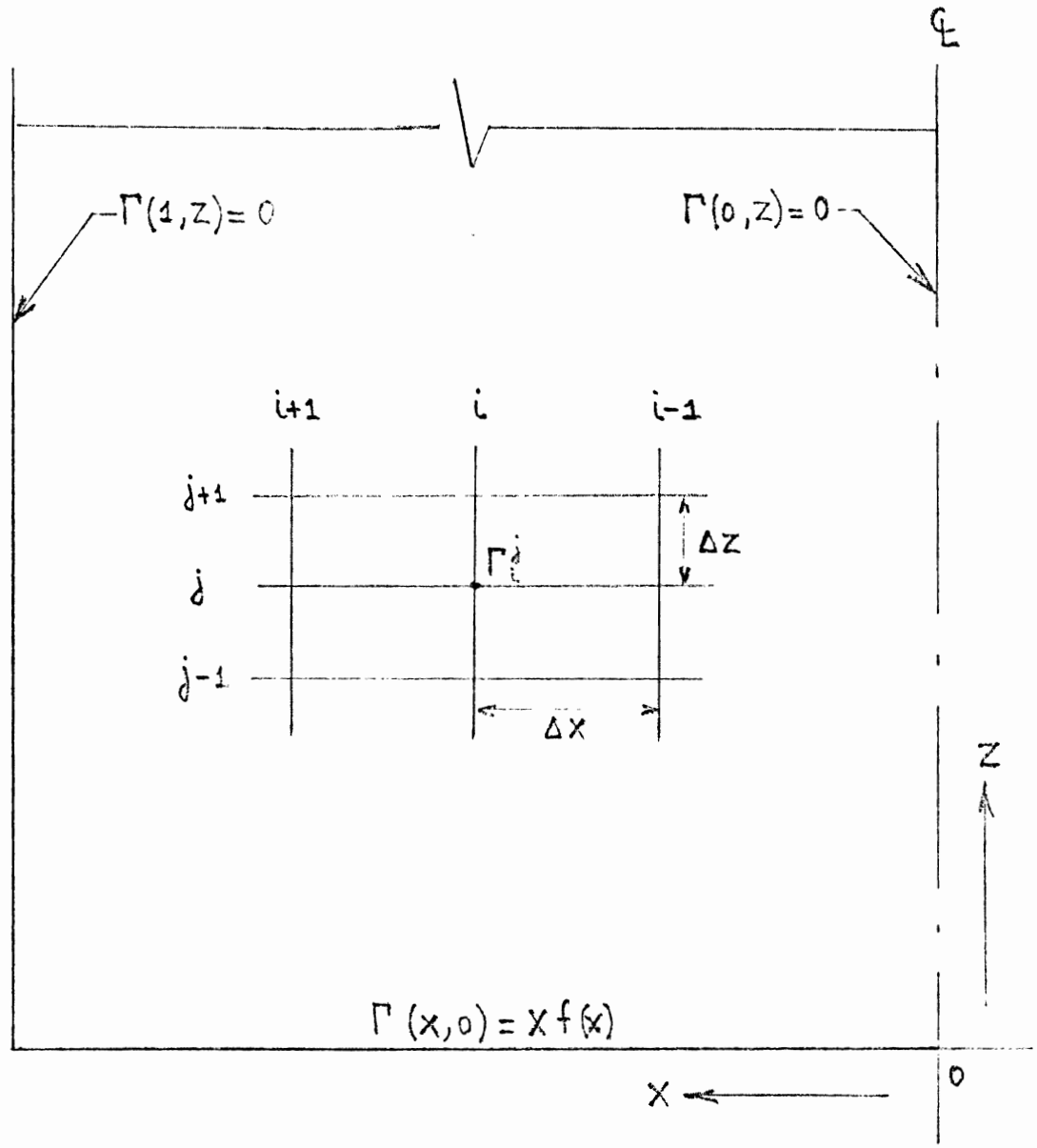
FIGURE 7 - GRID NOTATION AND BOUNDARY
CONDITIONS (Swirl Zone)

FIGURE 8 - RADIAL VELOCITY COMPONENT
VS
NOZZLE ANGLE
(Outlet of Plane - Free Jet Zone)
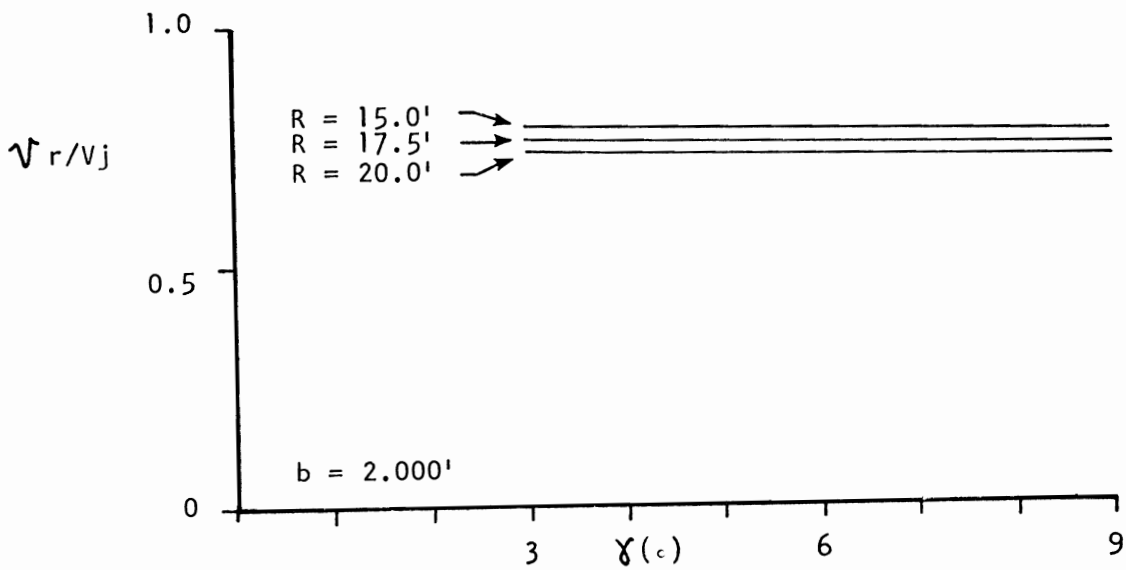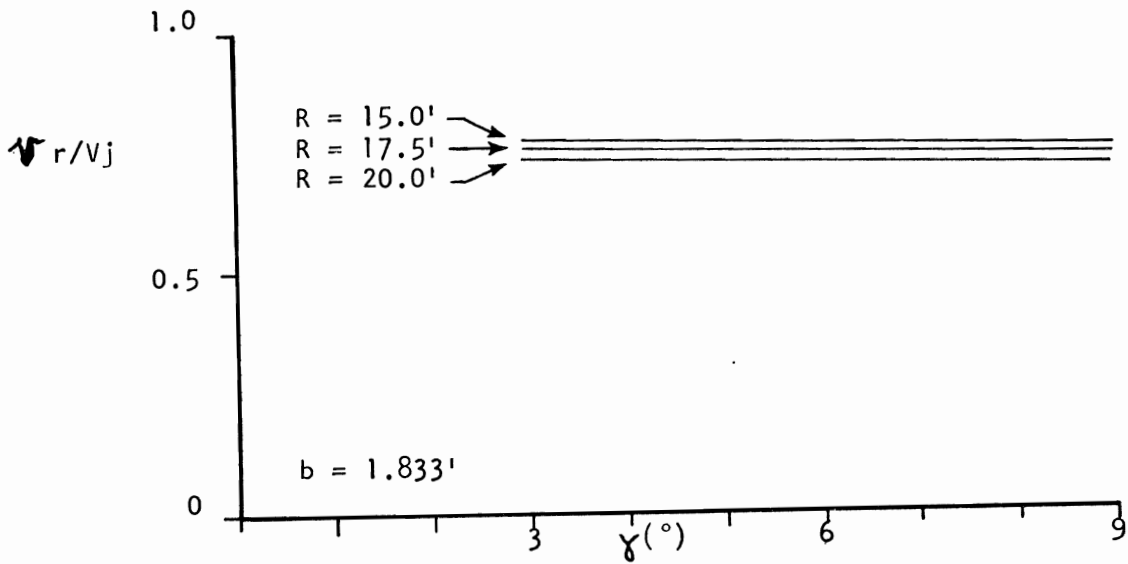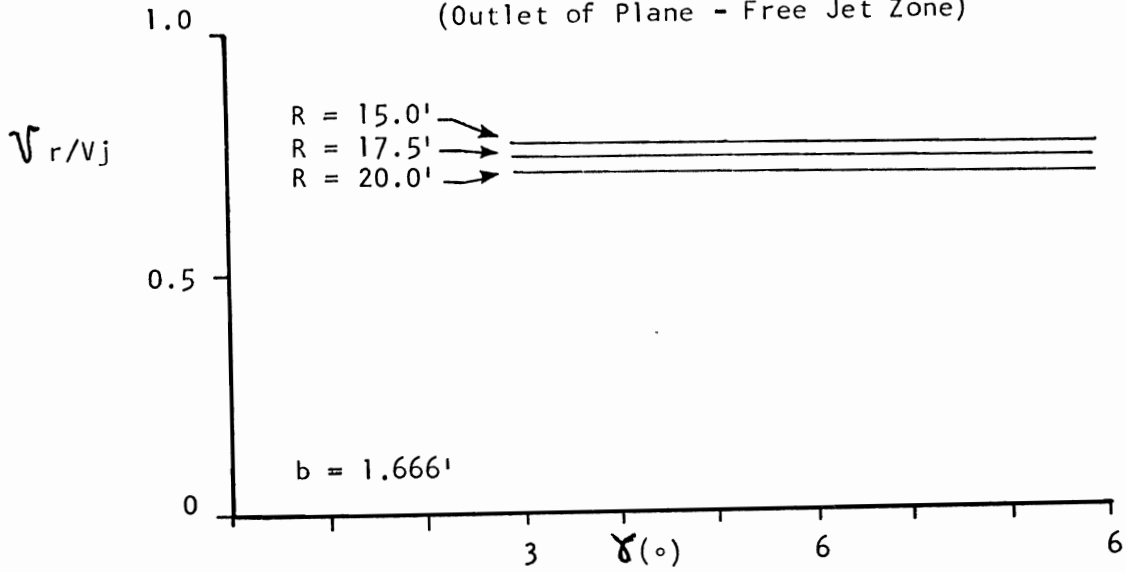
FIGURE 9 - TANGENTIAL VELOCITY COMPONENT
VS
NOZZLE ANGLE
(Outlet of Plane - Free Jet Zone)
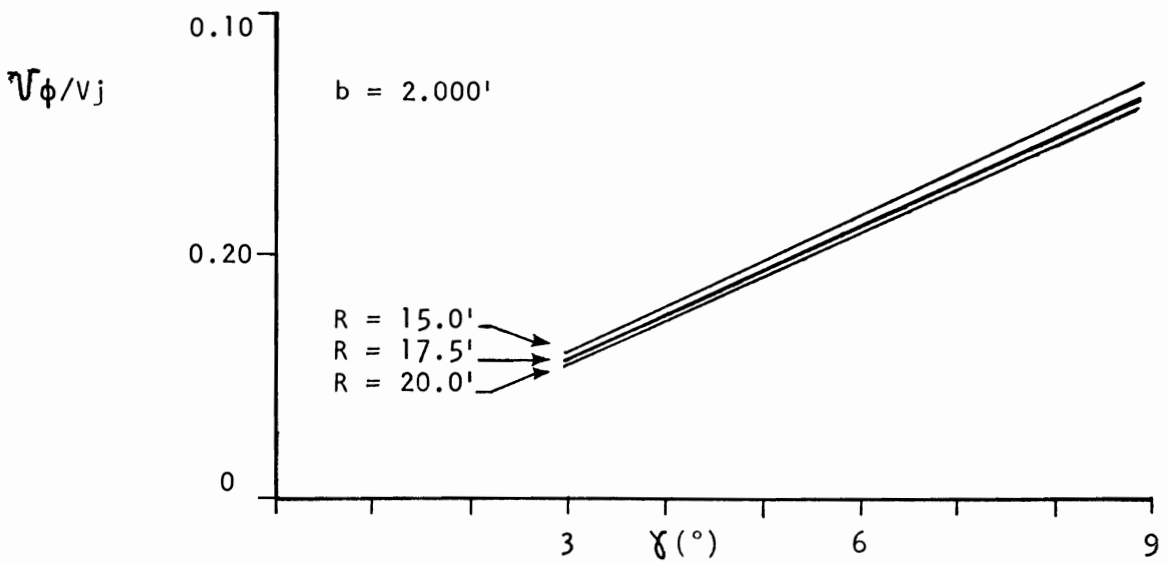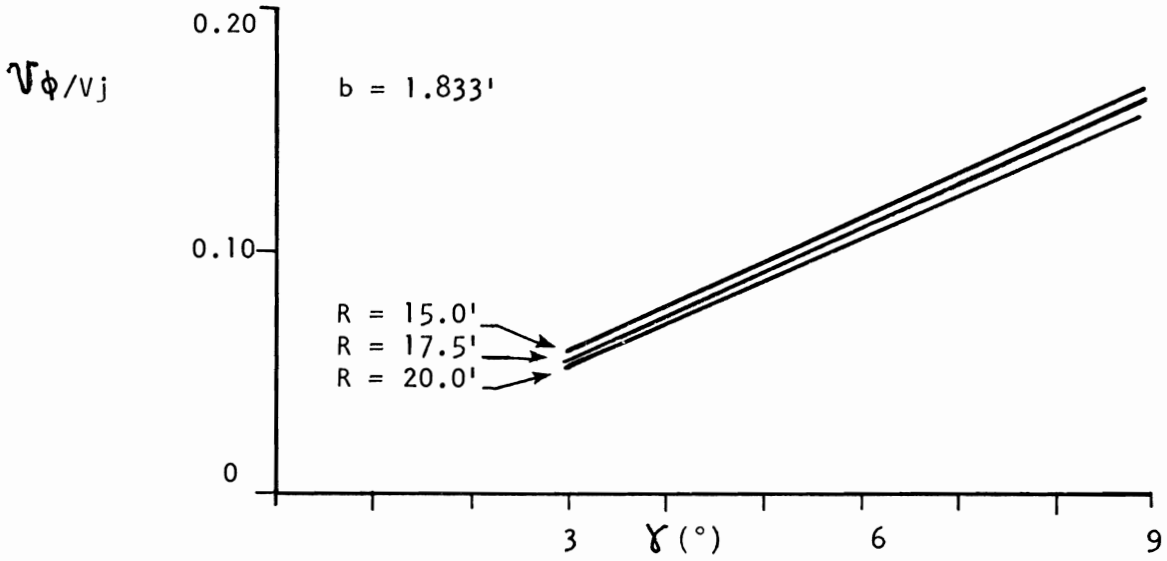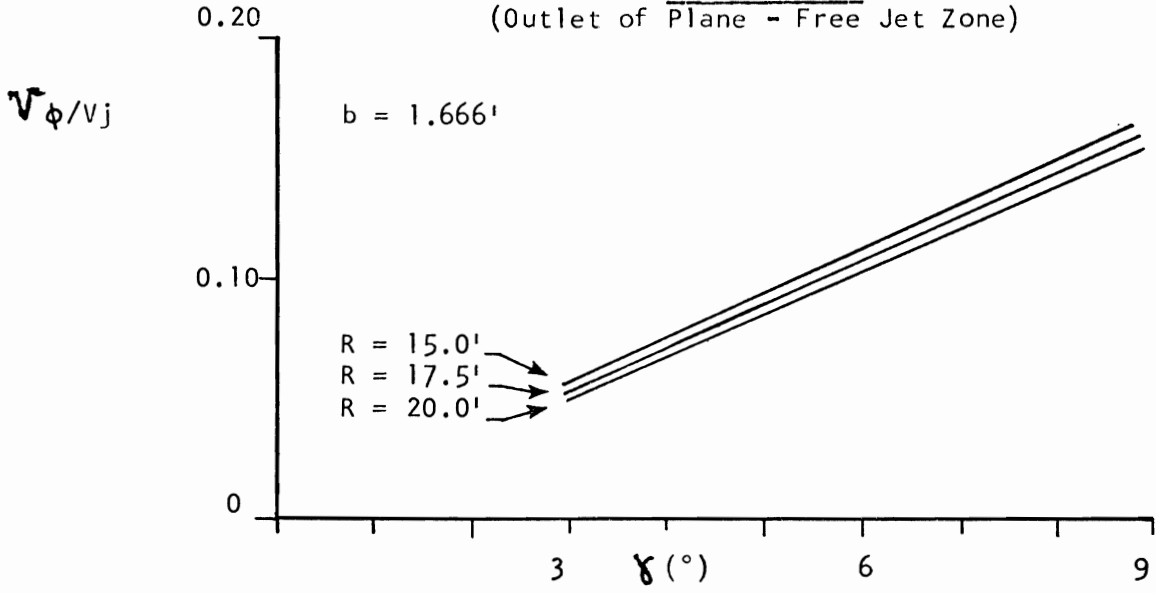
FIGURE 10 - <u>RADIAL VELOCITY FUNCTION</u>
(From the Outlet of Plane -
Free Jet Zone to the Inlet
of Vortex Zone)
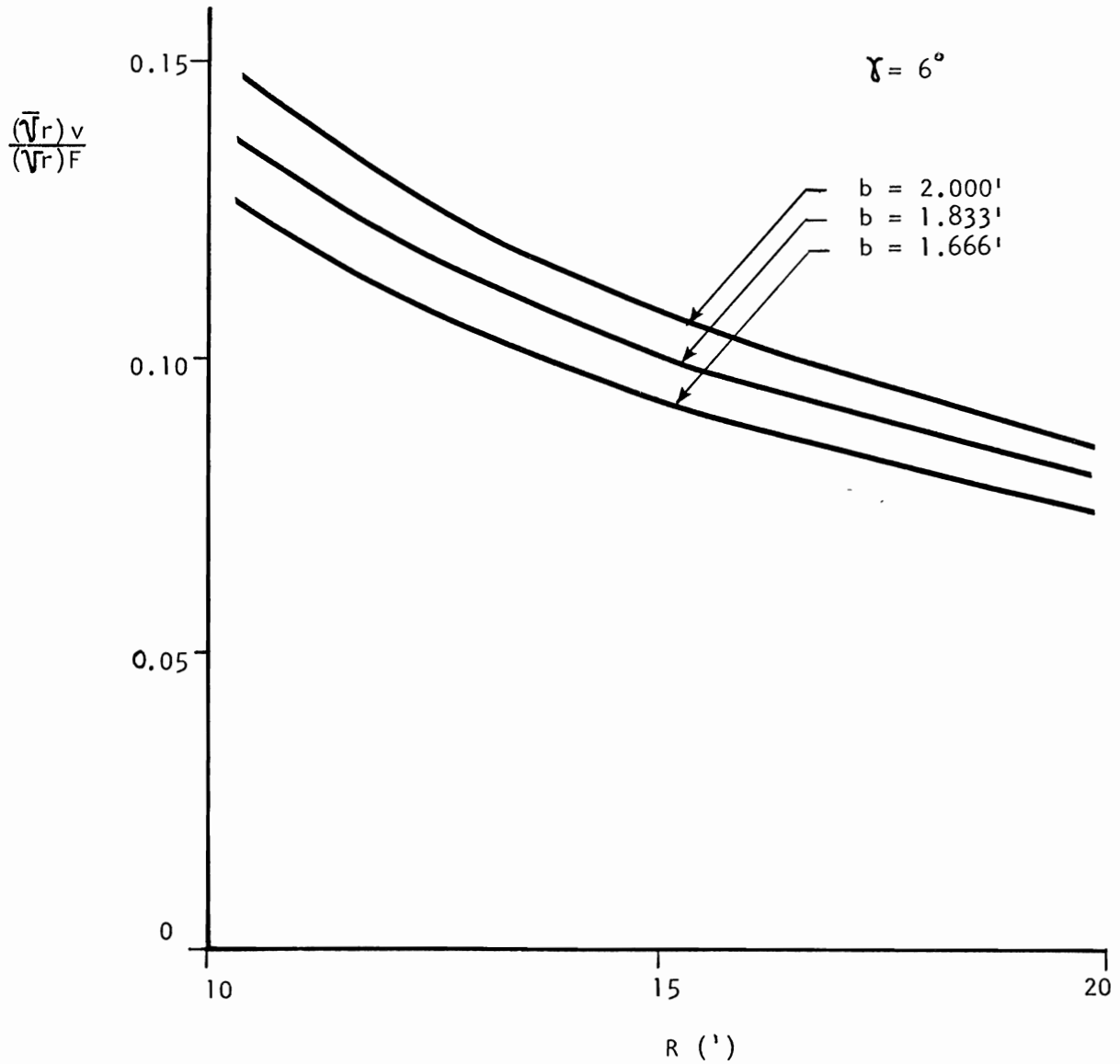
FIGURE 11 - β-FUNCTION VS ANGLE OF NOZZLE
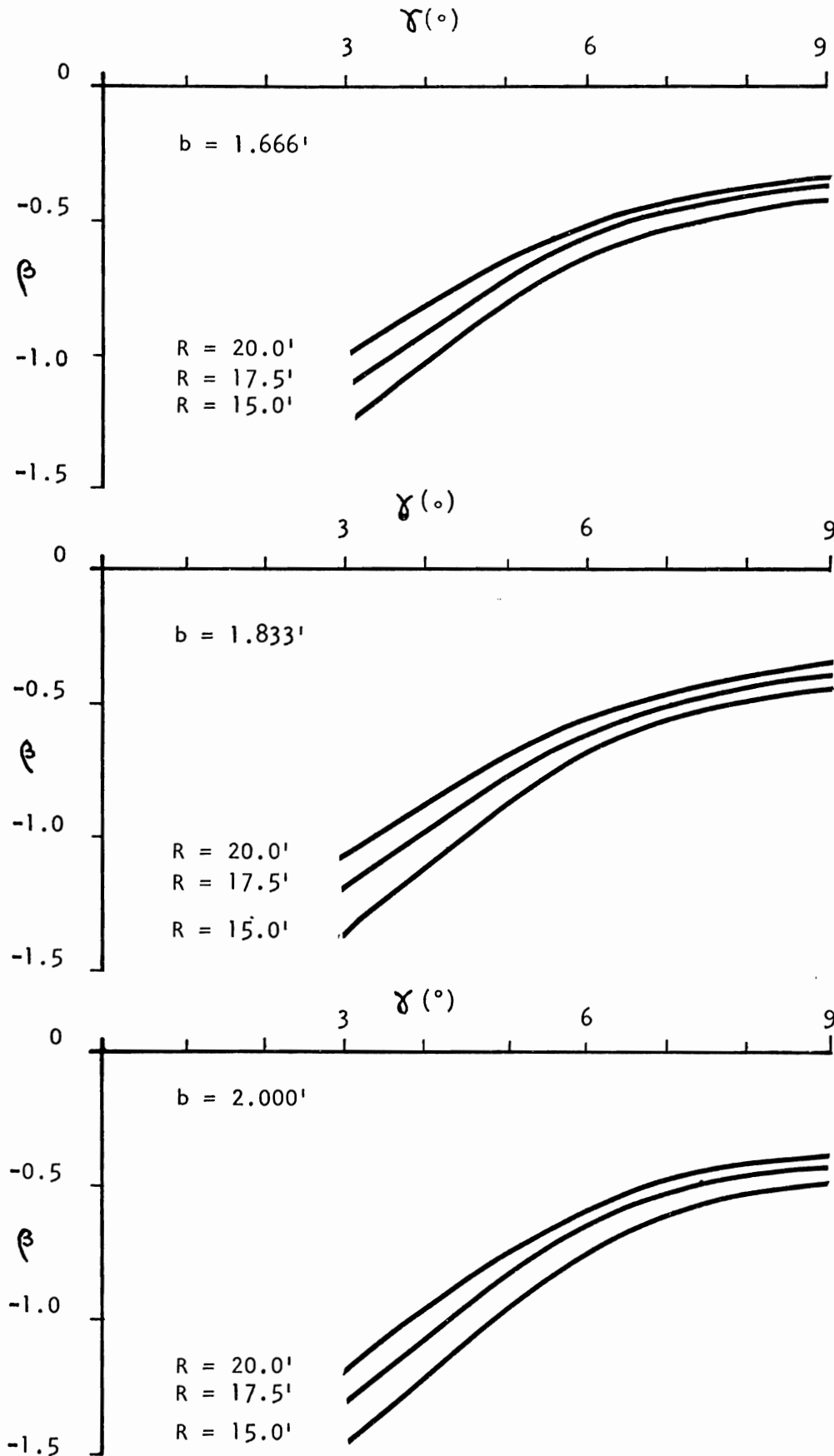
FIGURE 12 - TANGENTIAL VELOCITY DISTRIBUTION
(At Outlet of Vortex Zone)
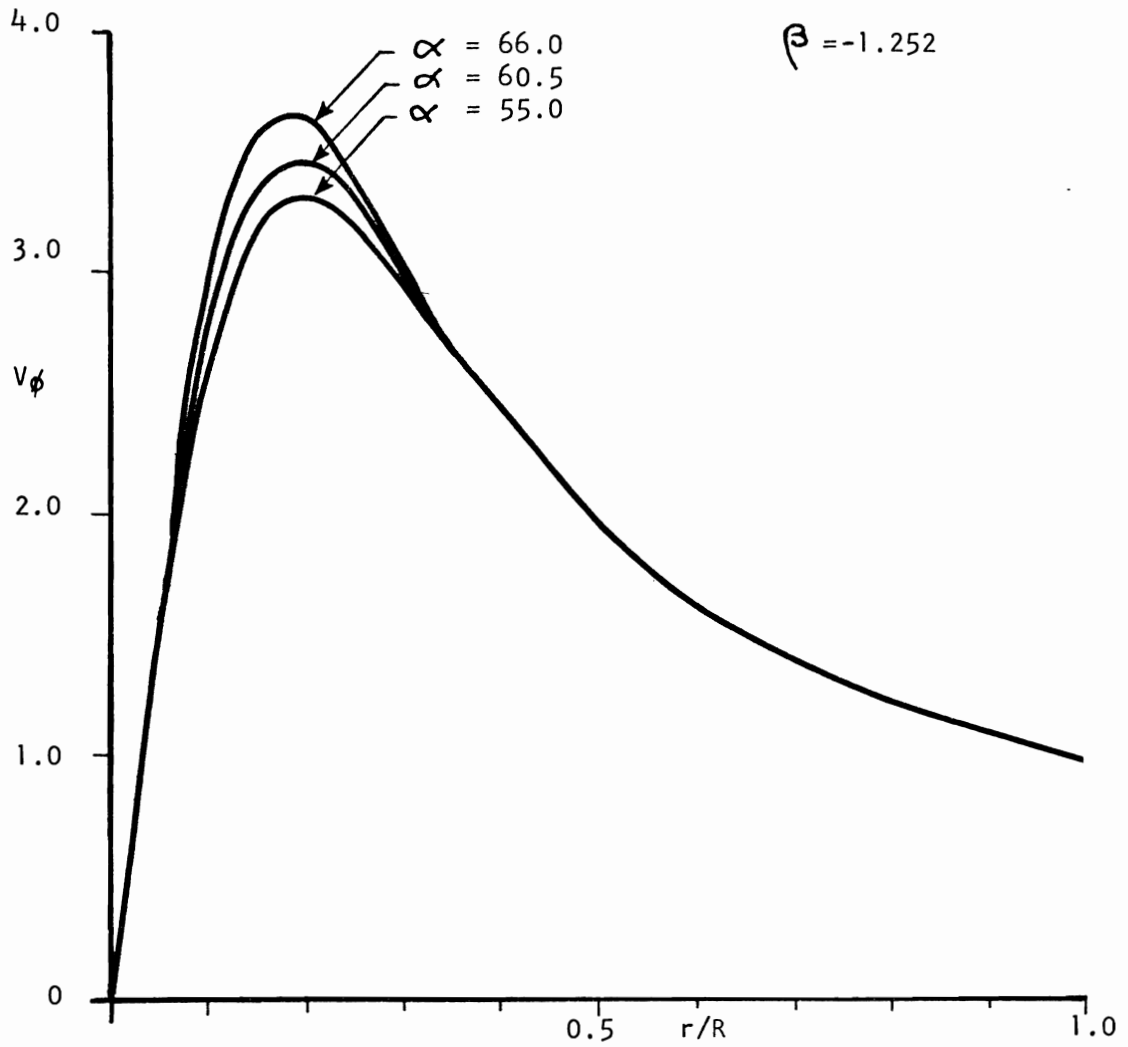
FIGURE 13 - <u>RADIAL VELOCITY DISTRIBUTION</u>
<u>(At Outlet of Vortex Zone)</u>
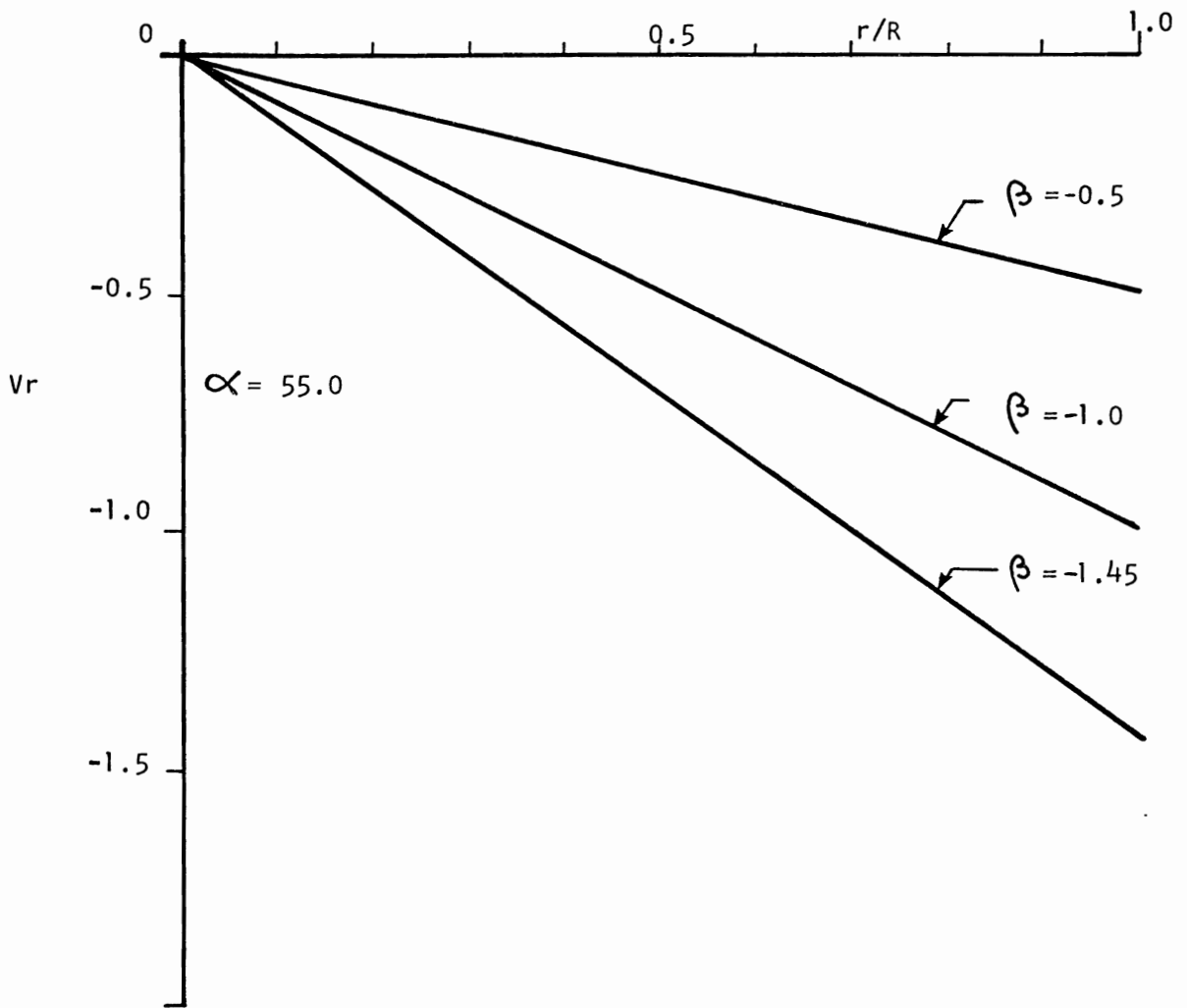
FIGURE 14 - <u>AXIAL VELOCITY DISTRIBUTION</u>
<u>(At Outlet of Vortex Zone: Z = 1)</u>
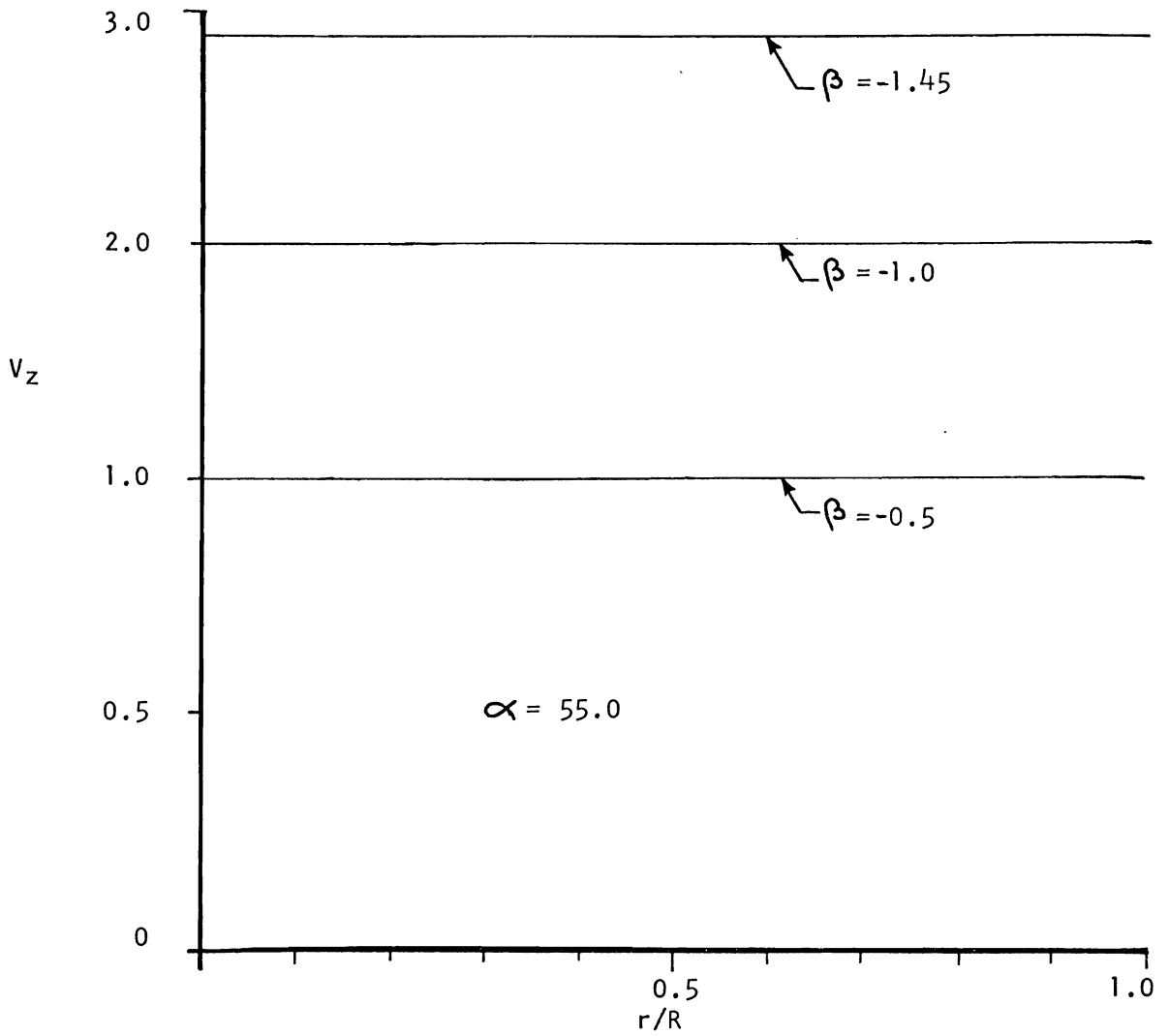
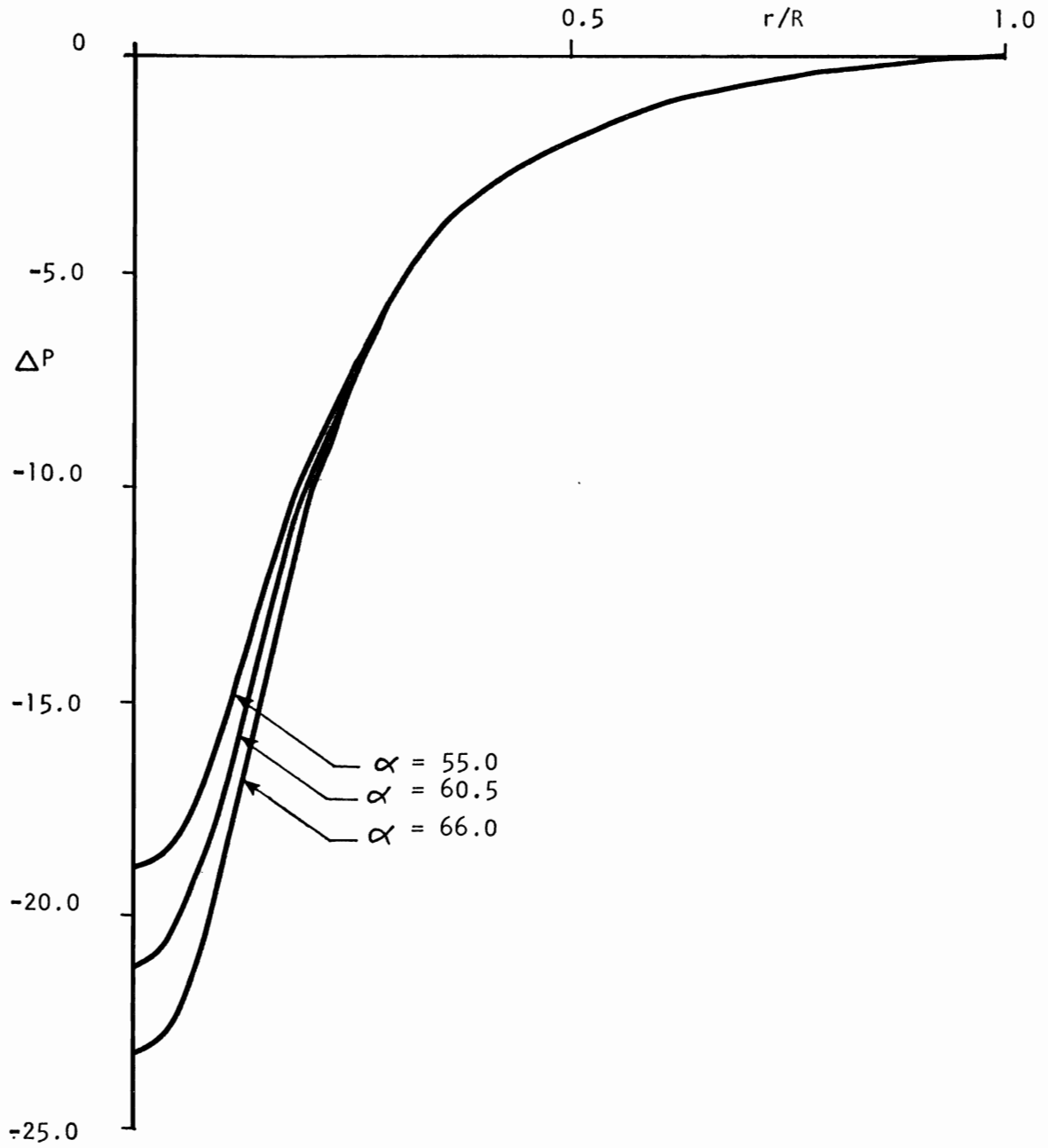FIGURE 15 - PRESSURE DIFFERENCE DISTRIBUTION
(Vortex Zone, Z = o, β = -1.252)

FIGURE 16 - <u>TANGENTIAL VELOCITY DISTRIBUTION</u>
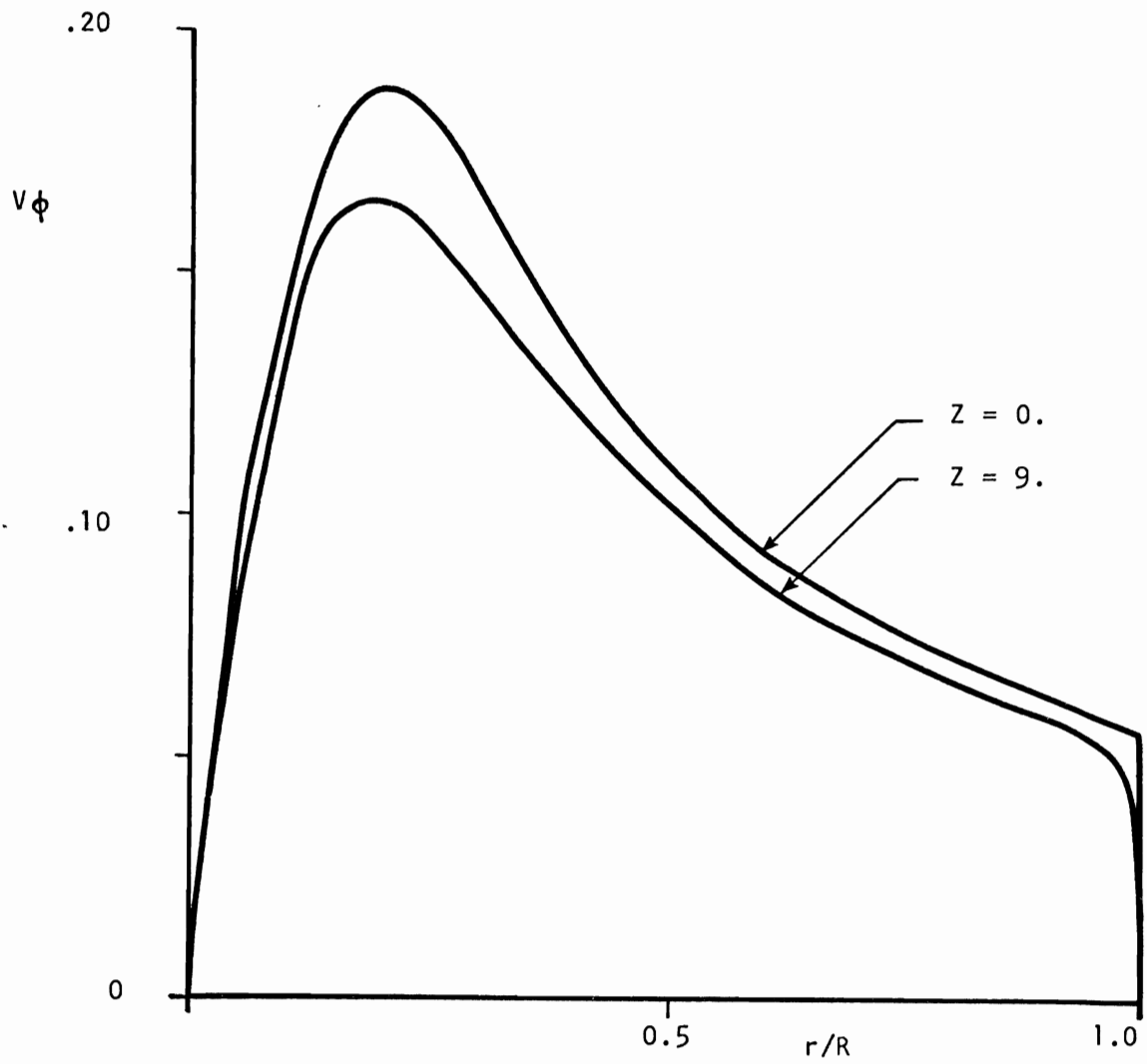<u>(Decaying Swirl Zone, $\alpha = 55.0$, $\beta = -1.252$)</u>

FIGURE 17 - TANGENTIAL VELOCITY DISTRIBUTION
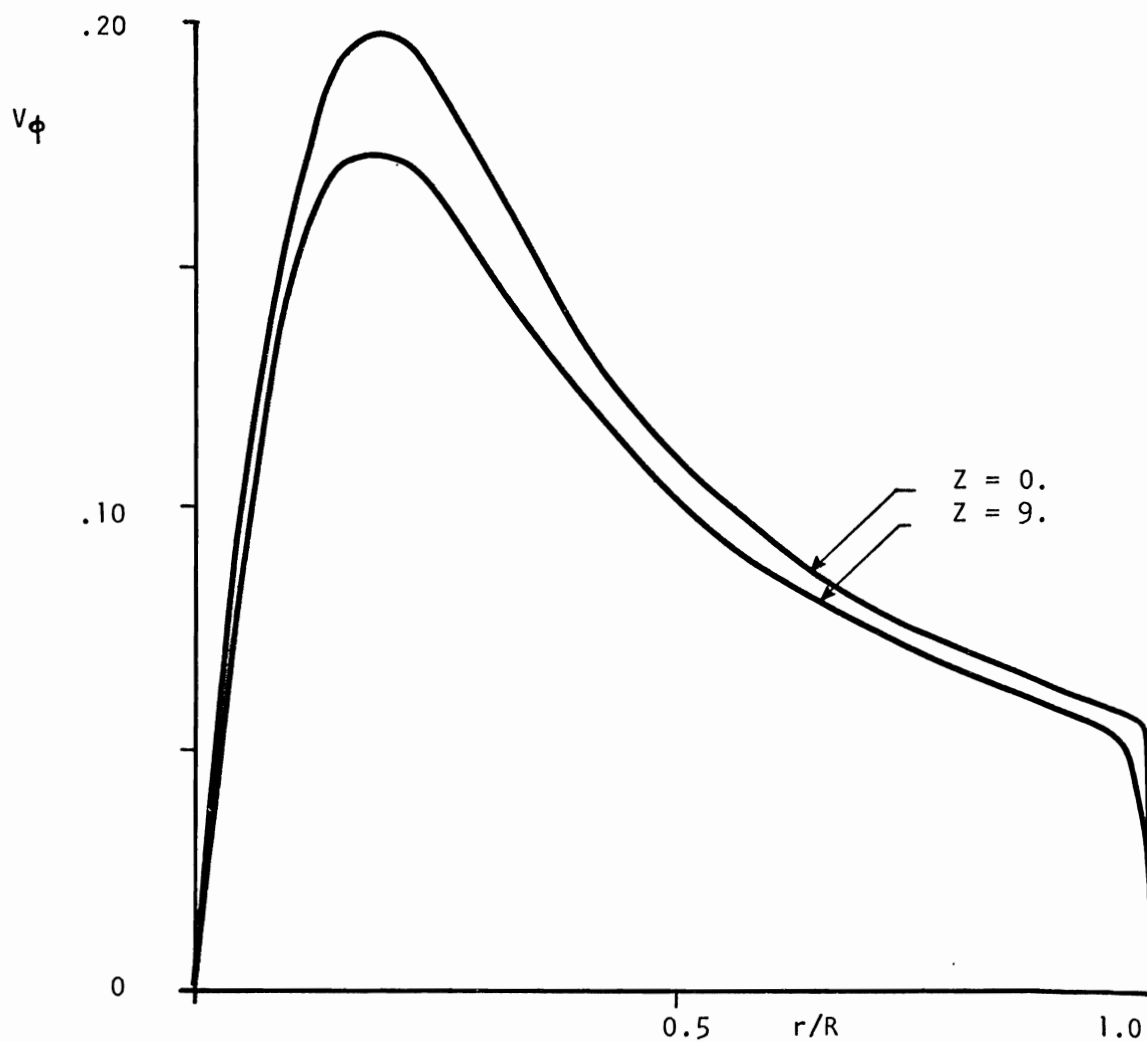(Decaying Swirl Zone, α = 60.0, β = -1.252)

FIGURE 18 - TANGENTIAL VELOCITY DISTRIBUTION
(Decaying Swirl Zone, α = 66.0, β=-1.252)